AD-A107 986 AIR FORCE INST OF TECH WRIGHT-PATTERSON AFB OH F/G 4/2
A DYNAMIC AND SYNOPTIC STUDY OF A WINTERTIME CYCLONE USING GEOS--ETC(U)
JUN 79 J A HALL
UNCLASSIFIED AFIT-CI-79-281T-S NL

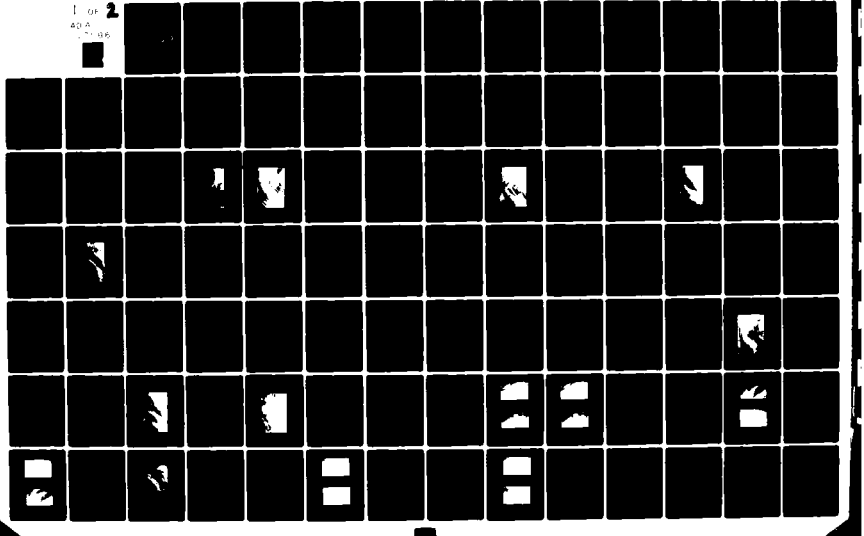

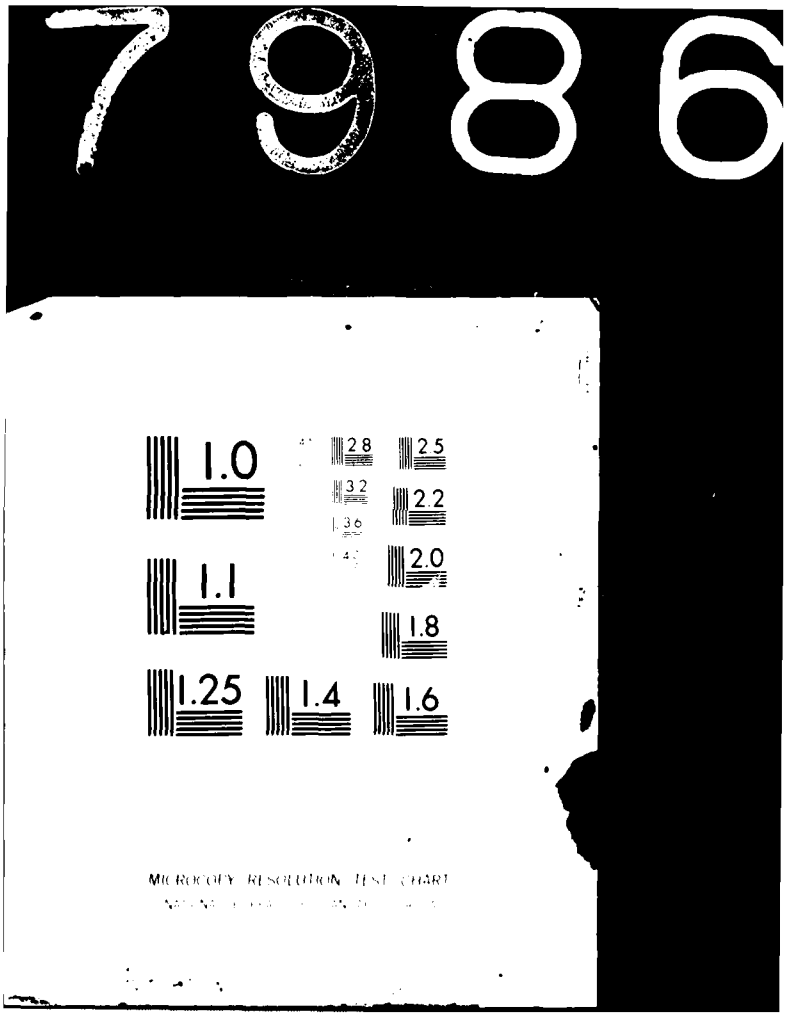
7986
1.0
1.1
1.25
1.4
1.6
2.8
3.2
3.6
2.5
2.2
2.0
1.8
MICROCOPY RESOLUTION TEST CHART

UNCLASS

SECURITY CLASSIFICATION OF THIS PAGE (When Data Entered)

REPORT DOCUMENTATION PAGE		READ INSTRUCTIONS BEFORE COMPLETING FORM
1. REPORT NUMBER 79-281T-S	2 GOVT ACCESSION NO AD-A107986	3 RECIPIENT'S CATALOG NUMBER
4. TITLE (and Subtitle) A Dynamic and Synoptic Study of a Wintertime Cyclone Using Geostationary and Polar Orbiting Satellite Data		5 TYPE OF REPORT & PERIOD COVERED THESIS/DISSERTATION
		6 PERFORMING ORG. REPORT NUMBER
7. AUTHOR(s) John Andrew Hall (1)		8 CONTRACT OR GRANT NUMBER(s)
9. PERFORMING ORGANIZATION NAME AND ADDRESS AFIT STUDENT AT: Univ of Utah		10 PROGRAM ELEMENT, PROJECT, TASK AREA & WORK UNIT NUMBERS
11. CONTROLLING OFFICE NAME AND ADDRESS AFIT/NR WPAFB OH 45433		12 REPORT DATE Jun 1979
		13 NUMBER OF PAGES 85
14. MONITORING AGENCY NAME & ADDRESS(if different from Controlling Office) LEVEL II		15. SECURITY CLASS. (of this report) UNCLASS
		15a. DECLASSIFICATION/DOWNGRADING SCHEDULE

16. DISTRIBUTION STATEMENT (of this Report)

APPROVED FOR PUBLIC RELEASE; DISTRIBUTION UNLIMITED

DTIC ELECTE DEC 1 1981 S D H

17. DISTRIBUTION STATEMENT (of the abstract entered in Block 20, if different from Report)

23 NOV 1981 Fredric C. Lynch

FREDRIC C. LYNCH, Major, USAF
Director of Public Affairs
Air Force Institute of Technology (ATC)
Wright-Patterson AFB, OH 45433

18. SUPPLEMENTARY NOTES

APPROVED FOR PUBLIC RELEASE: IAW AFR 190-17

19. KEY WORDS (Continue on reverse side if necessary and identify by block number)

20. ABSTRACT (Continue on reverse side if necessary and identify by block number)

ATTACHED

DD FORM 1 JAN 73 1473 EDITION OF 1 NOV 65 IS OBSOLETE UNCLASS

81 11 30 013 SECURITY CLASSIFICATION OF THIS PAGE (When Data Entered)

AD A107986

DTIC FILE COPY

A DYNAMIC AND SYNOPTIC STUDY OF A WINTERTIME CYCLONE USING GEOSTATIONARY AND POLAR ORBITING SATELLITE DATA

by

John Andrew Hall

A thesis submitted to the faculty of The University of Utah in partial fulfillment of the requirements for the degree of

Master of Science

Department of Meteorology

The University of Utah

June 1979

THE UNIVERSITY OF UTAH GRADUATE SCHOOL

SUPERVISORY COMMITTEE APPROVAL

of a thesis submitted by

John Andrew Hall

I have read this thesis and have found it to be of satisfactory quality for a master's degree.

4/5/79
Date

Elford G. Astling
Elford G. Astling
Chairman, Supervisory Committee

I have read this thesis and have found it to be of satisfactory quality for a master's degree.

4/5/79
Date

Kuo-Nan Liou
Member, Supervisory Committee

I have read this thesis and have found it to be of satisfactory quality for a master's degree.

4/6/79
Date

Julia N. Paegle
Julia N. Paegle
Member, Supervisory Committee

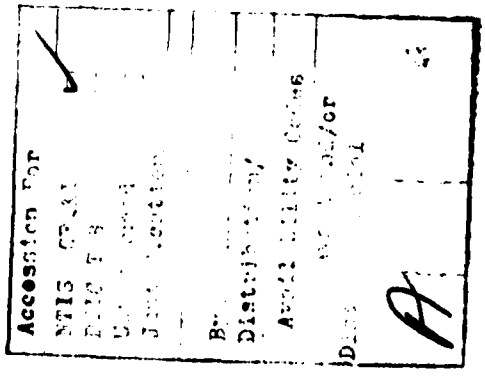

THE UNIVERSITY OF UTAH GRADUATE SCHOOL

FINAL READING APPROVAL

To the Graduate Council of The University of Utah:

I have read the thesis of John Andrew Hall in its final form and have found that (1) its format, citations, and bibliographic style are consistent and acceptable; (2) its illustrative materials including figures, tables, and charts are in place; and (3) the final manuscript is satisfactory to the Supervisory Committee and is ready for submission to the Graduate School.

April 5, 1979
Date

Elford G. Astling
Elford G. Astling
Member, Supervisory Committee

Approved for the Major Department

S. K. Kao
Chairman/Dean

Approved for the Graduate Council

James L. Clayton
Dean of The Graduate School

04
6-76

ABSTRACT

A detailed study was carried out for a mid-latitude cyclone that occurred over the United States from 20 to 22 February 1976. Results indicated that the Laplacian of thickness advection and differential vorticity advection by the nondivergent part of the flow, together with surface frictional effects, were the dominate mechanisms throughout the life history of the cyclone. The storm underwent rapid development when the ascending motions, produced by these forcing functions, were nearly coincident and exhibited no vertical tilt in the lee of the Rocky Mountains. When the cyclone reached maturity, the strongest thermal and vorticity effects at mid-tropospheric levels advanced eastward ahead of the most intense frictional components at low levels. When the cyclone began to occlude, sinking motion was contributed by differential vorticity advection by the divergent part of the flow at low levels. This effect decreased the strong rising motion due to friction and eventually produced a shallow layer of subsidence that extended into the occluded system.

Numerical computations of three dimensional trajectories illustrated the importance of low level moisture flow and the development of intense convective activity within the warm air sector of the cyclone. Comparisons of atmospheric trajectories with visible and infrared imagery from satellites showed good agreement with cloud fields and vertical motions. Also, the numerical computations showed the importance of low level flow in determining the configuration of cloud fields on a synoptic scale.

TABLE OF CONTENTS

LIST OF FIGURES

ACKNOWLEDGEMENTS

My sincere thanks and appreciation go to Dr. Elford G. Astling for the guidance and assistance he gave me during this thesis preparation. I am also very grateful to Capt. Paul T. Nipko for the cooperation and advice with the numerous computer programs used to prepare this paper, and to my fellow students who helped significantly.

Special thanks go to my wife, Eleanor, for her love and encouragement and to my sons, Jeffrey, Scott and Tyler for their patience and understanding during this research period.

This research was supported by the Air Force Geophysics Laboratory, Bedford, Massachusetts under Grant F19628-78-C-0130.

CHAPTER I

INTRODUCTION

Many synoptic scale systems traversed the North American continent during the 1975-76 winter season. One system of particular interest was a midlatitude cyclone that went through a complete life cycle between 20 and 22 February 1976 as it moved eastward across the United States. During this period, conventional meteorological data were enhanced with visible and infrared imagery from two geostationary satellites and multi-spectral radiation observations from the Nimbus VI polar orbiting satellite. These observations were combined to carry out a detailed investigation of physical and dynamical mechanisms related to the evolution of the cyclone.

Vertical motions were computed at four consecutive map times from a numerical model which defined important mechanisms such as thermal and vorticity effects, stable and convective type of latent heat release, surface friction and orographic effects. Mathematical formulation of the model also included both the divergent and non-divergent components of the horizontal wind. Vertical motions were computed and used to obtain three-dimensional trajectories. The computational results of partitioned vertical velocities by the various forcing functions together with atmospheric trajectories were compared with cloud and precipitation fields in an attempt to explain the evolution of the storm.

Several meteorological parameters were obtained from satellite observations. Evolution of cloud fields were followed in film loops of infrared images from geostationary satellites. The vertical extent of convective clouds in the warm air sector of the cyclone were estimated from enhanced infrared images. Also, surface and cloud top temperatures were compared with infrared measurements from a polar orbiting satellite.

CHAPTER II

DATA AND ANALYSIS TECHNIQUES

The data used in this study were accumulated from a number of sources. Input parameters for the vertical motion calculations were available on magnetic tapes from the National Center for Atmospheric Research (NCAR). This information was originally prepared by the National Meteorological Center (NMC) for operational use and was eventually sent to NCAR for research purposes. The data included a four layer moisture field obtained from radiosonde observations, seven layers of geopotential heights, and sea level pressure analyses. Details about modification of these data for use in this study will be discussed later in this chapter.

Numerical radiometer data from an experiment onboard the Nimbus VI satellite were provided by the National Space Science Data Center at Goddard Space Flight Center. This information was analyzed for specific quantities of temperature fields.

In addition to meteorological data in digital formats, synoptic charts at selected levels for some parameters from the National Weather Service were also used as well as geostationary satellite imagery for visual identification and detailed analyses of the synoptic system. The standard isobaric analysis depicted the amplitude of trough-ridge patterns and relative movements during 12 hour synoptic time intervals. Other supplemental charts such as the National Radar Summary and six

hourly precipitation amounts provided detailed information for time periods less than 12 hours for the February 1976 cyclone.

Conventional Meteorological Data

Analyses of Radiosonde data at four successive 12 hour intervals were the primary sources for tropospheric values of relative humidity and geopotential height fields. Objective analysis of geopotential heights by NMC provided data for 850, 700, 500, 400, 300, and 200 mb surface. These data were transformed from a Northern Hemispheric 65 X 65 octogonal grid with a mesh size of 320 km (at 35°N) onto a rectangular grid centered over the United States with a mesh size of 2.5° latitude by 3.6° longitude. A 16 point Bensel interpolation scheme, described by Jenne (1970), was employed to extract the data onto a 27 X 15 grid array that is shown in Fig. 1. This array encompasses the area from 25°N to 60°N latitudes and between 146.6°W to 54.6°W longitudes.

It was found that the NMC 1000 mb analyses for 0000 and 1200 GMT on 21 February 1976 did not have sufficient detail near the cyclone center. Only radiosonde data had been used in the NMC analyses and, as a result, the geopotential height gradients were smoothed and artificially reduced. To overcome this problem, the 1000 mb height fields for these two map times were derived from sea level pressure charts where the observational data network is more than four times as dense and permits more detailed analyses. Tabulations at one-half the grid resolution were carried out for the sea level pressure analysis. Then a five point smoothing routine was applied to the sea level pressure to obtain values for the 27 X 15 grid array. The centered difference routine used was,

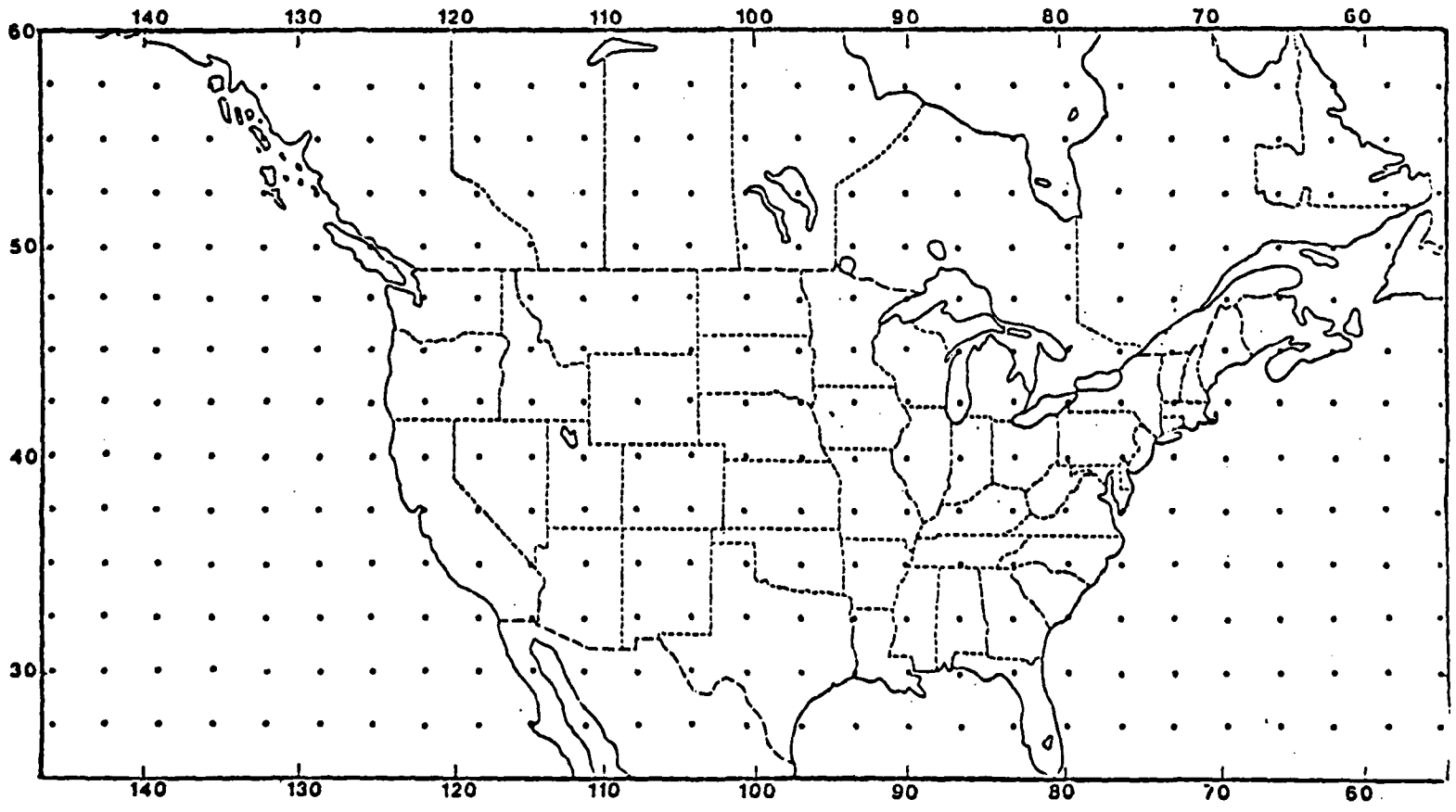

Figure 1. Horizontal Grid used in the numerical computation over a 27 X 15 domain with a 3.6° longitude and 2.5° latitude mesh size.

$$P_{i,j} = (P_{i-1/2,j} + P_{i+1/2,j} + P_{i,j-1/2} + P_{i,j+1/2} + 2P_{i,j})/6 \quad (1)$$

where $P_{i,j}$ is the sea level pressure and i and j represent the grid array of 27 longitude points by 15 latitude points.

The hypsometric equation was used to compute the 1000 mb geopotential heights from sea level pressures at each grid point using

$$Z_{1000} = Z_{SL} + \frac{R_d \overline{T}}{g} \ln \frac{P_{SL}}{P_{1000}} \quad (2)$$

where $Z_{SL} = 0$ for the geopotential height at sea level, R_d is the gas constant, g is acceleration of gravity, P_{SL} is the sea level pressure, $P_{1000} = 1000$ mb, and $\overline{T}$ is the mean virtual temperature of the layer. Values for $\overline{T}$ were approximated by 1000 mb temperatures from the NMC data tapes. Computed 1000 mb heights by this method produced more detail in the structure of the lower troposphere than the original NMC analysis.

Radiosonde data for all four map times were analyzed for relative humidity at the surface, 850, 700 and 500 mb levels. Because of the unreliable radiosonde measurements of moisture at low temperatures, relative humidities at 300 mb were extrapolated from lower levels and the moisture at 200 mb was assumed to be negligible. The number of conventional radiosonde data was very limited over the adjacent oceanic regions. An NMC analysis of mean layer moisture for three tropospheric layers, each with a depth approximately equal to 1/3 of the pressure height from the boundary layer to the tropopause, provided information over the water surfaces. Data from these sources, together with radar summaries and GOES imagery, were subjectively blended in an analysis for the entire grid array. The 72 hour infrared film loop also

provided useful information about these fields, particularly those that were not easily discernible on the conventional charts. Relative humidites were interpolated to the nearest percent to the 27 X 15 grid array.

Nimbus VI Satellite Measurements

Nimbus VI was launched on 12 June 1975 in a sun-synchromous polar orbit at an altitude of 1100 km. The satellite provided nearly complete data coverage with approximately three successive orbital passes over the continental United States each day near local noon and local midnight (Nimbus VI User's Guide, 1975). Successive orbits crossed the equator with 26.8 degrees of longitude separation and with an orbital period of 107 minutes (Fig. 2).

One radiometer instrument on board Nimbus VI provided useful data for the study -- a High Resolution Infrared Radiation Sounder (HIRS). The experiment provided data that were transformed with an objective analysis program from scan points along the orbital path to the 27 X 15 grid array shown in Fig. 1.

The basic concept of the objective analyses was similar to a scheme described by Cressman (1959) except that a preliminary analysis was omitted. Scan points from the satellite orbital swath that were within a prescribed radius of influence of each grid point were applied to the analyses. A weighting factor was defined for each satellite data point for each s-th observation near the grid point according to the following formulation;

$$W_s = \frac{D^2-d^2}{D^2+d^2} \qquad (3)$$

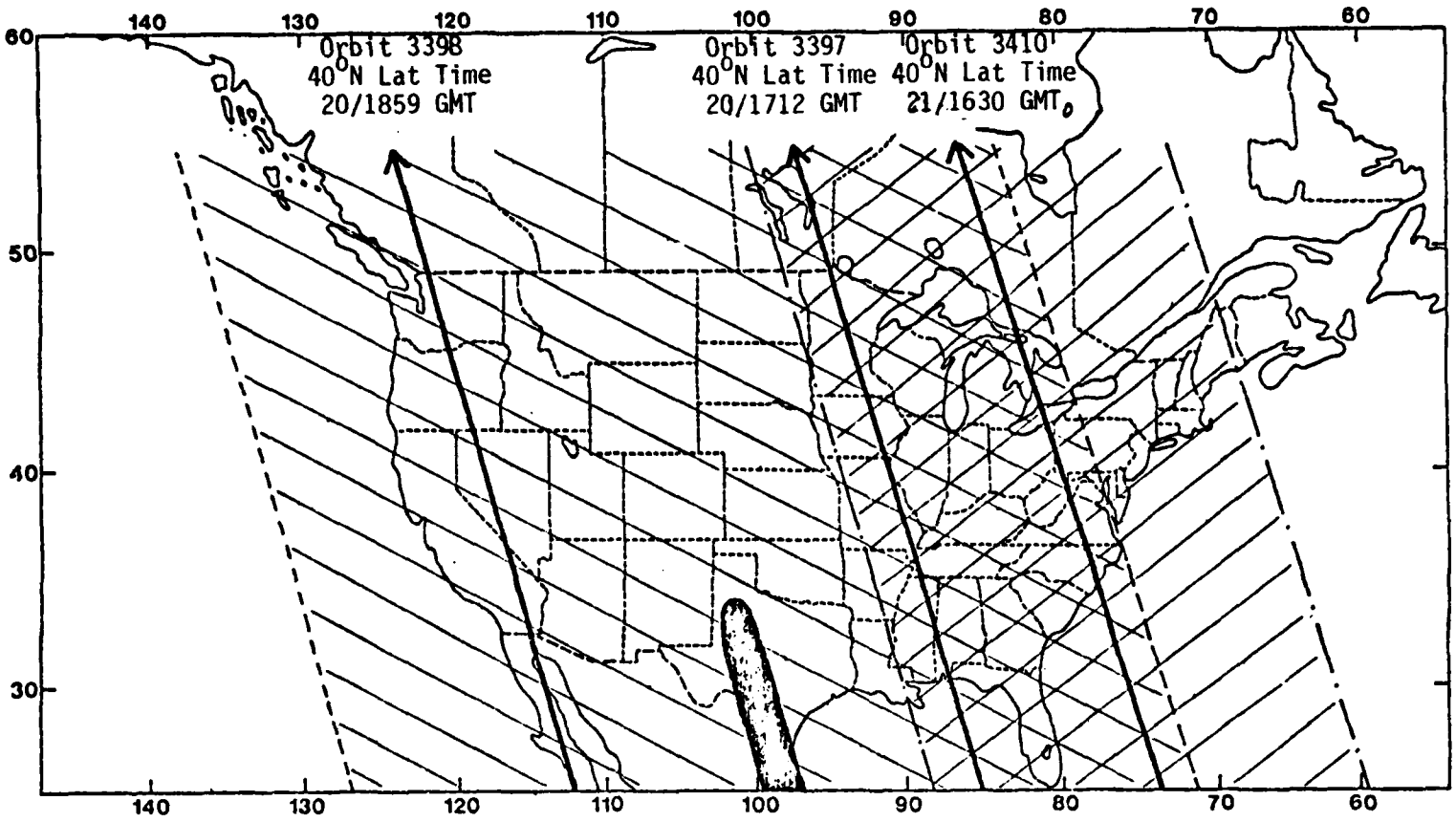

Figure 2. Orbital passes for the HIRS experiment from Nimbus VI.

where D is the radius of influence and d is the distance from the grid point to the location of the satellite observation. It is obvious that if the satellite observation was coincident with the grid point, the weighting function was unity, because d=0. Whenever d approached the value of D, the weighting function went to zero. Several experiments were carried out with different values of D to find the most suitable size for the objective analysis. It was found that scale size down-to-near the subsynoptic portion of the spectrum were adequately represented when D=2.5° latitude or 277 km.

Objectively analyzed satellite radiance values (R_{ij}) at each grid point (i,j) were then obtained from the following relationship

$$R_{ij} = \frac{\sum_s W_s R_s}{\sum_s W_s} \qquad (4)$$

where R_s is a satellite radiance measurement at each s-th scan point within a distance d of the grid point. For the Nimbus VI data, satellite scan point population for each grid point along the orbital track averaged approximately 110 for the HIRS data around each grid point. This analysis produced smoothed and interpolated satellite data that represented atmospheric systems with scale sizes comparable to the ones resolved by the conventional meteorological data.

Sensors in the HIRS experiment measured radiance values in 17 spectral bands between 3.7 μm and 15 μm. Planck's law was used to infer blackbody radiative temperatures for all of the channels. In this study only the 11 μm window channel was used to detect surface or cloud top temperatures depending on the amount of cloudiness. Data from the other spectral bands for this synoptic system were not considered in this

investigation. The HIRS instrument scanned along a line perpendicular to the subsatellite track with a resolution that ranged from approximately 24 km at nadir to 45 km at 36.9° viewing angles. A contiguous geographical sampling was obtained from 21 scan spot elements on each side of the subsatellite track, when Nimbus VI passed over the United States .

GOES Visible and Infrared Imagery

Visible and infrared imagery from two geostationary satellites were also used to supplement conventional meteorological information. High resolution images were taken by both SMS-2 (Synchronous Meteorological Satellite) and GOES-1 (Geostationary Operational Environment Satellite) at 30 minute intervals throughout the period of study. SMS-2 was launched on 6 February 1975 into a geostationary equatorial orbit and was positioned over 135°W longitude at an altitude of 36,000 km. GOES-1 was launched on 16 October 1975 in a similar orbital configuration except its equatorial subsatellite point was at 75°W. Good coverage was provided by SMS-2 when the mid-latitude cyclone was located over the western United States and by GOES-1 when the storm moved into the Midwest.

Both geostationary satellites were equipped with a Visible and Infrared Spin Scan Radiometer (VISSR) which provided imagery from a reflected solar radiation channel during daytime, and from a thermal infrared radiation channel for both day and night. The resolution was 1.2 km for the visible channel and 12 km for the 10.5 to 12.5 μm channel over the central United States. The high resolution imagery simultaneously observed meteorological motion fields that could be discerned from movie loops of the infrared imagery.

Vertical Motions

Vertical motion for all four map times were computed using a diagnostic multi-level balance model described by Krishnamurti (1968). This model computes partitional omegas by various forcing functions to permit an investigation of the complex dynamical and physical mechanisms. Six forcing functions were determined by Astling (1976) to be significant for a mid-latitude cyclone in another case study and were used for this February 1976 cyclone.

The omega equation used was

$$\nabla^2\sigma\omega + f^2 \frac{\partial^2\omega}{\partial p^2} = f \frac{\partial}{\partial p} J(\psi,\zeta_a) + \pi\nabla^2 J(\psi,\theta)$$

$$+ f \frac{\partial}{\partial p} g \frac{\partial}{\partial p} \left(\frac{\partial \tau_y}{\partial x} - \frac{\partial \tau_x}{\partial y}\right) - \frac{R}{C_p p} \nabla^2 H_L$$

$$- f \frac{\partial}{\partial p} (\nabla\chi\cdot\nabla\zeta_a) - \pi\nabla^2(\nabla\chi\cdot\nabla\theta) \qquad (5)$$

where the terms on the R.H.S. are respectively, (1) differential vorticity advection by the non-divergent part of the wind, (2) Laplacian of thermal advection by the non-divergent part of the wind, (3) frictional stresses at the surface, (4) latent heat release, (5) differential advection of vorticity by the divergent part of the wind. The symbols in Eq. (5) are defined in the Appendix.

Starting with input data for 20 February 1200 Z, when the system formed, intensified and decayed. Using the model, numerical methods were applied to solve three equations for ω, $\frac{\partial\psi}{\partial t}$ and χ. These included a non-linear system of partial differential equation that solved for the vertical motion from the omega equation, the mass continuity equation that yielded the velocity potential, and the vorticity equation

which yielded the stream function tendency $\frac{\partial \psi}{\partial t}$. Values of omega were obtained at the 900, 700, 500 and 300 mb pressure surfaces. These motions were than compared with both geostationary and polar orbiting satellites, and were used to explain synoptic scale patterns in this cyclone.

The boundary condition at the 100 mb surface was $\omega=0$ and at 1000 mb it was defined as

$$\omega_{1000} = - g \frac{1000}{RT} [J(\psi,h) - \nabla\chi\cdot\nabla h] \qquad (6)$$

where h is the surface terrain height and the other variables are defined in Eq. (5). This represents vertical motions induced by orographic effects. Values for h over the 27 X 15 grid domain were obtained from a report by Berkofsky and Bertoni (1960) at 1° latitude-longitude grid intervals.

Atmospheric Trajectory Computations

The three dimensional velocity vectors, that were computed from the nonlinear balanced omega equation, were integrated over the four map times to obtain trajectories of atmospheric motion. Horizontal wind components at five levels (1000, 800, 600, 400 and 200 mb) were interpolated with vertical velocities at four intermediate levels (900, 700, 500 and 300 mb) to carry out the integration at four hour time steps.

The method of trajectory computations was accomplished by starting at the initial time of 1200 GMT 20 February. Wind data for only this map time were used to start the integration and to locate the air parcel's position P_1 after 4 hours according to the following

relationship:

$$\mathbb{P}_1 = \mathbb{P}_0 + \tilde{\mathbb{V}}_0 \, \Delta t \tag{7}$$

where the vector $\mathbb{P}_0 = \mathbb{P}(x_0, y_0, p_0, t_0)$ represents the initial position of an air parcel at time t_0 in three dimensional space with pressure as the vertical coordinate. $\tilde{\mathbb{V}}_0$ is the velocity vector which is interpolated to $\mathbb{P}_0$ and Δt is the time increment of four hours.

The method for interpolating the velocity vector can be obtained at an arbitrary point from the wind components at the grid points from the following relation:

$$\begin{aligned}\tilde{\mathbb{V}}(t_0) = \{&[(1-\Delta x)\mathbb{V}_{x,y,p}(t_0) + \Delta x \, \mathbb{V}_{x+1,y,p}(t_0)](1-\Delta y) \\ &+ [(1-\Delta x)\mathbb{V}_{x,y+1,p}(t_0) + \Delta x \, \mathbb{V}_{x+1,y+1,p}(t_0)]\Delta y\} \, (1-\Delta p) \\ &+ \{[(1-\Delta x)\mathbb{V}_{x,y,p+1}(t_0) + \Delta x \, \mathbb{V}_{x+1,y,p+1}](1-\Delta y) \\ &+ [(1-\Delta x)\mathbb{V}_{x,y+1,p+1}(t_0) + \Delta x \, \mathbb{V}_{x+1,y+1,p+1}]\Delta y\} \, \Delta p\end{aligned} \tag{8}$$

where the subscripts denote grid points in the (x,y,p) coordinate system. Interpolations of the velocity vector with respect to time used the following expression:

$$\tilde{\mathbb{V}}(t_1) = \tilde{\mathbb{V}}(t_0) \tag{9}$$

for the 0 to 4 hour trajectory, and

$$\tilde{\mathbb{V}}(t_2) = (\tilde{\mathbb{V}}(t_0) + \tilde{\mathbb{V}}(t_3))/2 \tag{10}$$

for the 4 to 8 hour trajectory where t_3 represents the next 12 hour map

time. Then the 8 to 12 hour trajectory was computed from

$$\tilde{W}(t_3) = \tilde{W}(t_3) \tag{11}$$

the velocities at subsequent time increments can be obtained by repeating this interpolation scheme as defined in Eqs. 7 to 11. The air parcel trajectory for the i-th time step was obtained from

$$\mathbb{P}_{i+1} = \mathbb{P}_i + \tilde{W}(t_i)\ \Delta t \tag{12}$$

where $\mathbb{P}_i$ is the location of the trajectory at the previous time step and $W(t_i)$ is the velocity vector interpolated to $\mathbb{P}_i$.

It should be noted that other trajectory computational schemes might yield better results (Reap, 1972; Danielsen, 1973) especially if subjective hand analyses of the wind field are used. However, the method used in this study is more suitable to the output data from the three dimensional diagnostic computations. It was found that atmospheric trajectories computed by the method described here compared favorably with cloud motions in film loops of infrared imagery from the geostationary satellite. The results will be discussed in Chapter V.

CHAPTER III

SYNOPTIC SITUATION

The midlatitude cyclone moved eastward across the United States during the period from 19 to 23 February 1976. The storm entered the western United States as a very weak surface low which began to redevelop over the Great Basin early on 19 February. By 0000 GMT on 20 February, the surface low moved to the Utah and Colorado border and had a central pressure of 998 mb. At this time, a low level trough formed down stream in the lee of the Rockies in northeastern Colorado, while the upper level trough was still somewhat to the west over northeastern Nevada. This feature is often found with cyclones that move across the intermountain region of the western United States (Palmén and Newton, 1969). The system was relatively dry with precipitation confined to a limited area over northern Colorado and southern Wyoming. The evaluation of this synoptic system will be described in this chapter for time sequences of twelve hours when upper air data were available from 1200 GMT 20 February to 0000 GMT 22 February 1976.

Synoptic Situation at 1200 GMT 20 February 1976

By this time, the surface cyclone merged with the lee side trough to form a single low pressure center in southeastern Colorado as shown in Figure 3a. The 500 mb trough was associated with pronounced cold air advection and deepened over western Colorado (Fig. 3b). Precipitation that accompanied this system formed north and west of the surface

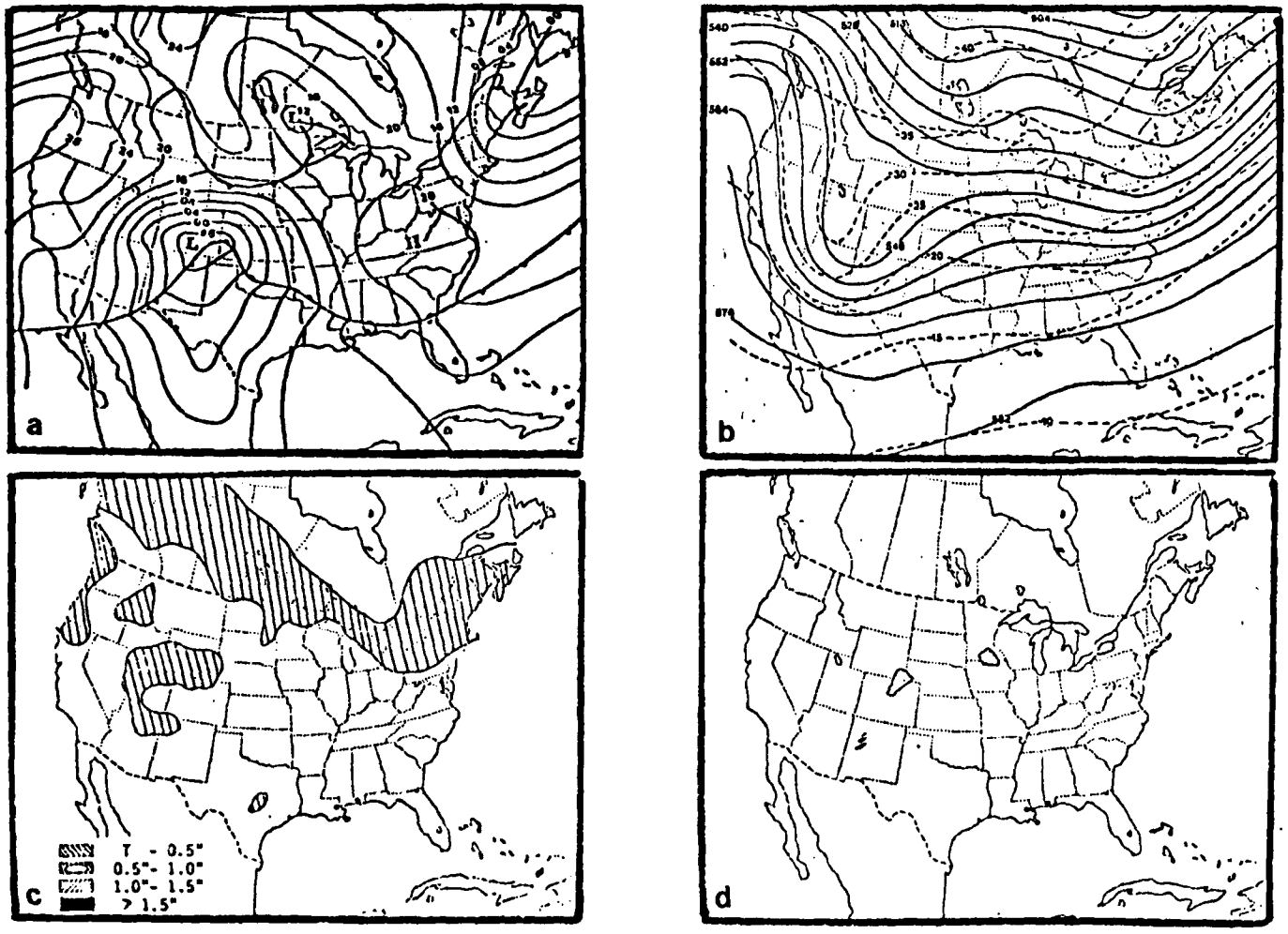

Figure 3. (a) Sea level pressure analysis, (b) 500 mb analysis, (c) 6 hour precipitation amounts, and (d) radar summary at 1200 GMT 20 February 1976.

low as revealed in 6 hourly precipitation accumulations and on the radar summary in Figs. 3c and 3d. An extensive area south of the surface low remained relatively dry. The 850 and 500 mb relative humidity analyses together with the infrared imagery from the geostationary satellite depicted this important feature in Fig. 4.

GOES-East Visual Imagery at 2000 GMT 21 February 1976

The severe weather formed by 2300 GMT 20 February 1976. Depicted in Fig. 5 is the visual imagery for 2000 GMT. This imagery illustrates the intrusion of moisture at low level and the dry tongue at all levels. The western cloud band extending from eastern Kansas to central Oklahama exhibits small cellular cumulus which developed into the organized line of severe weather identified in the next section (Point 1). The area south of the surface low is very dry and with the strong gradient extending into west central Texas, many stations reported blowing dust. Point 2 in Fig. 5 is a area of blowing dust.

Synoptic Situation at 0000 GMT 21 February 1976

By the second map time Fig. 6a shows the surface low had moved into central Kansas, with no deepening of the low pressure center. The 500 mb trough progressed eastward into southeastern Colorado (Fig. 6b). The area of strong pressure gradients west of the surface low 12 hours earlier, underwent noticeable strengthening and extended to the north of the system. A warm front stretched eastward from the low center to Kansas and southeast into Mississippi and across the Gulf of Mexico to the Florida Pennisula. A cold front reached southward through the Big Bend area of Texas and then southwest to Baja California.

By this map time, thunderstorm activity and significant amounts of

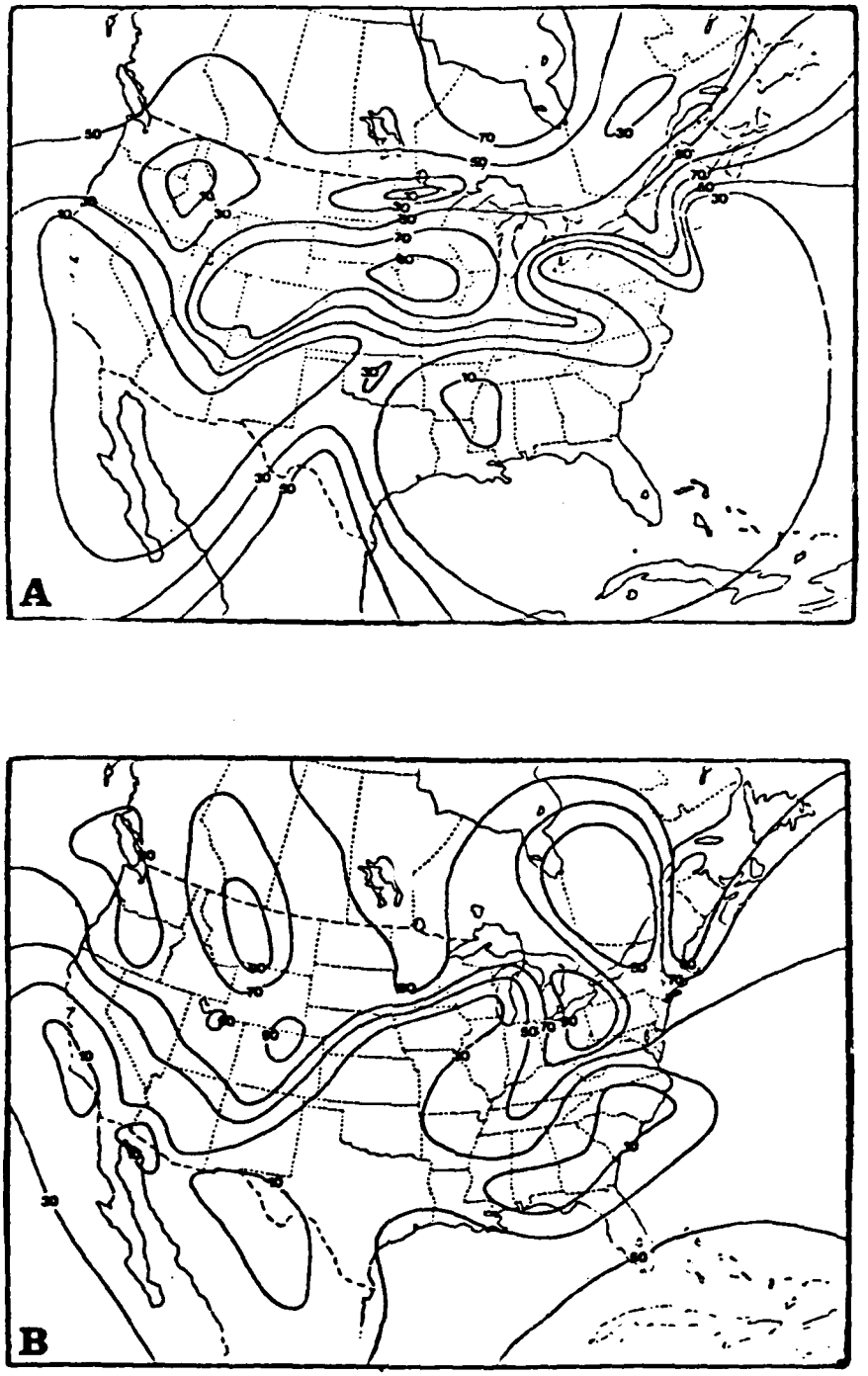

Figure 4. Relative humidity analysis at 1200 GMT 20 February 1976 for the (a) 500 mb level and (b) 850 mb level.

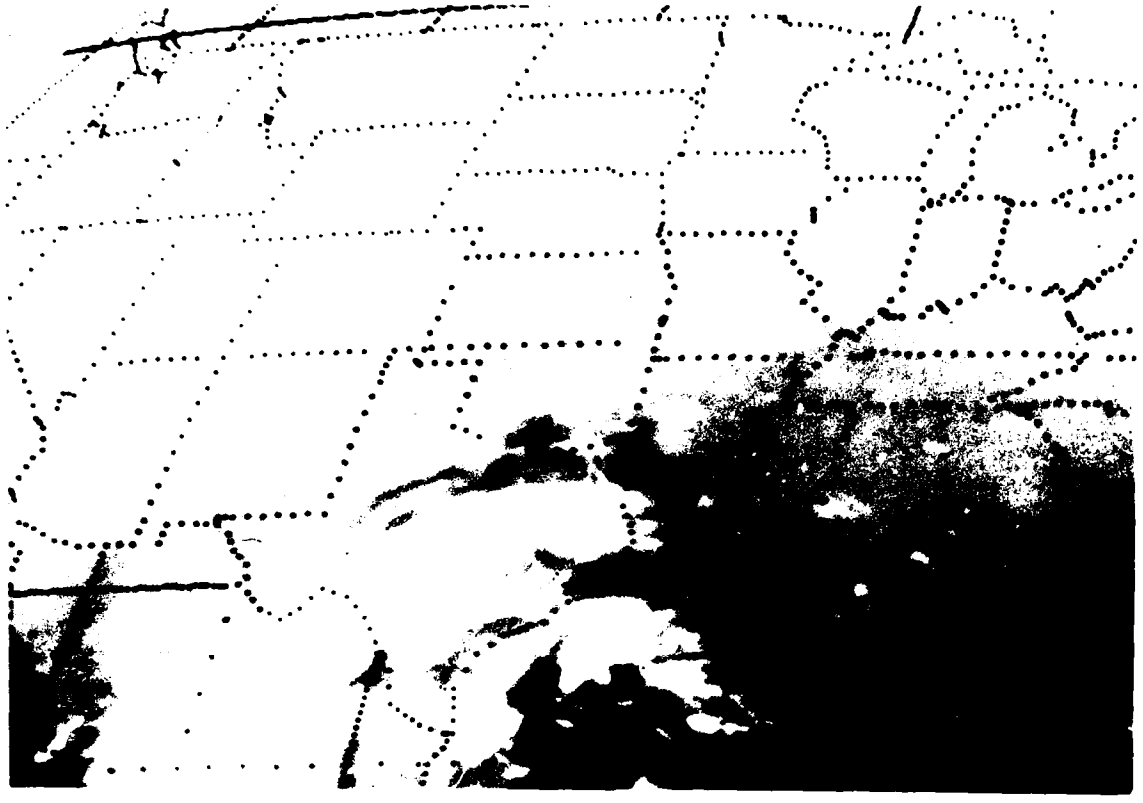

Figure 4. (c) GOES-East infrared satellite imagery at 1200 GMT 20 February 1976.

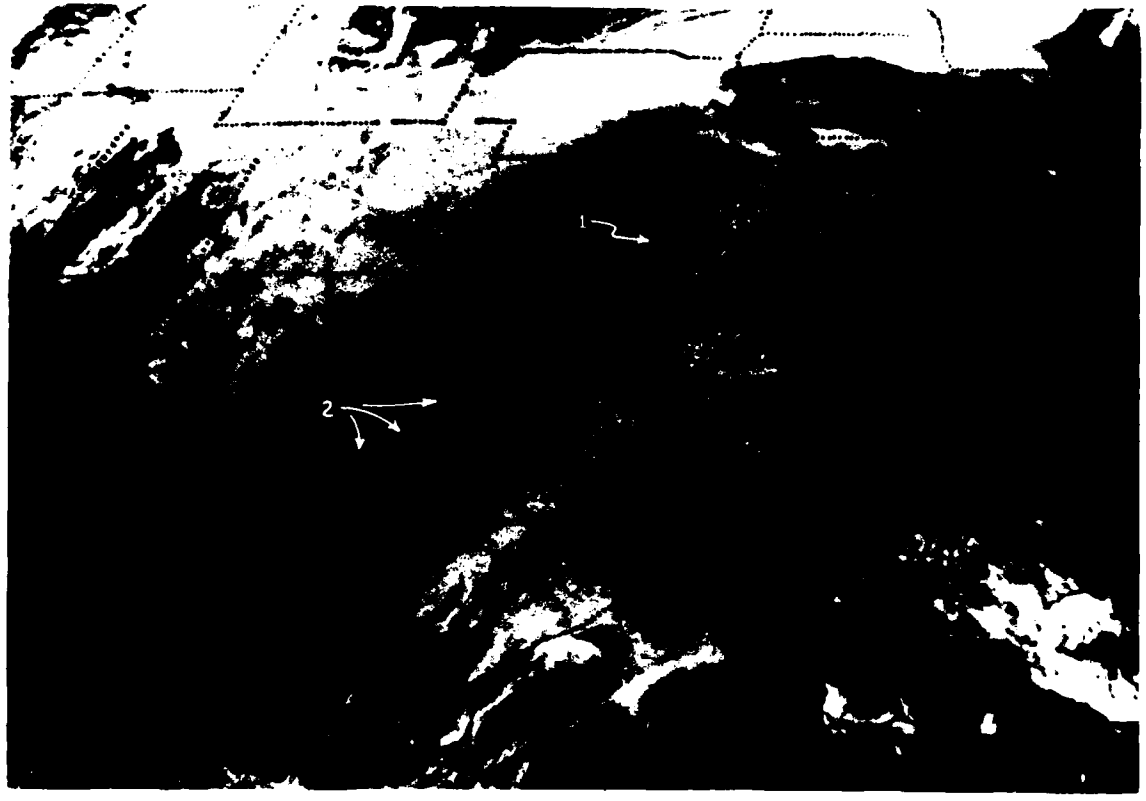

Figure 5. GOES-East visual satellite imagery at 2000 GMT 20 February 1976.

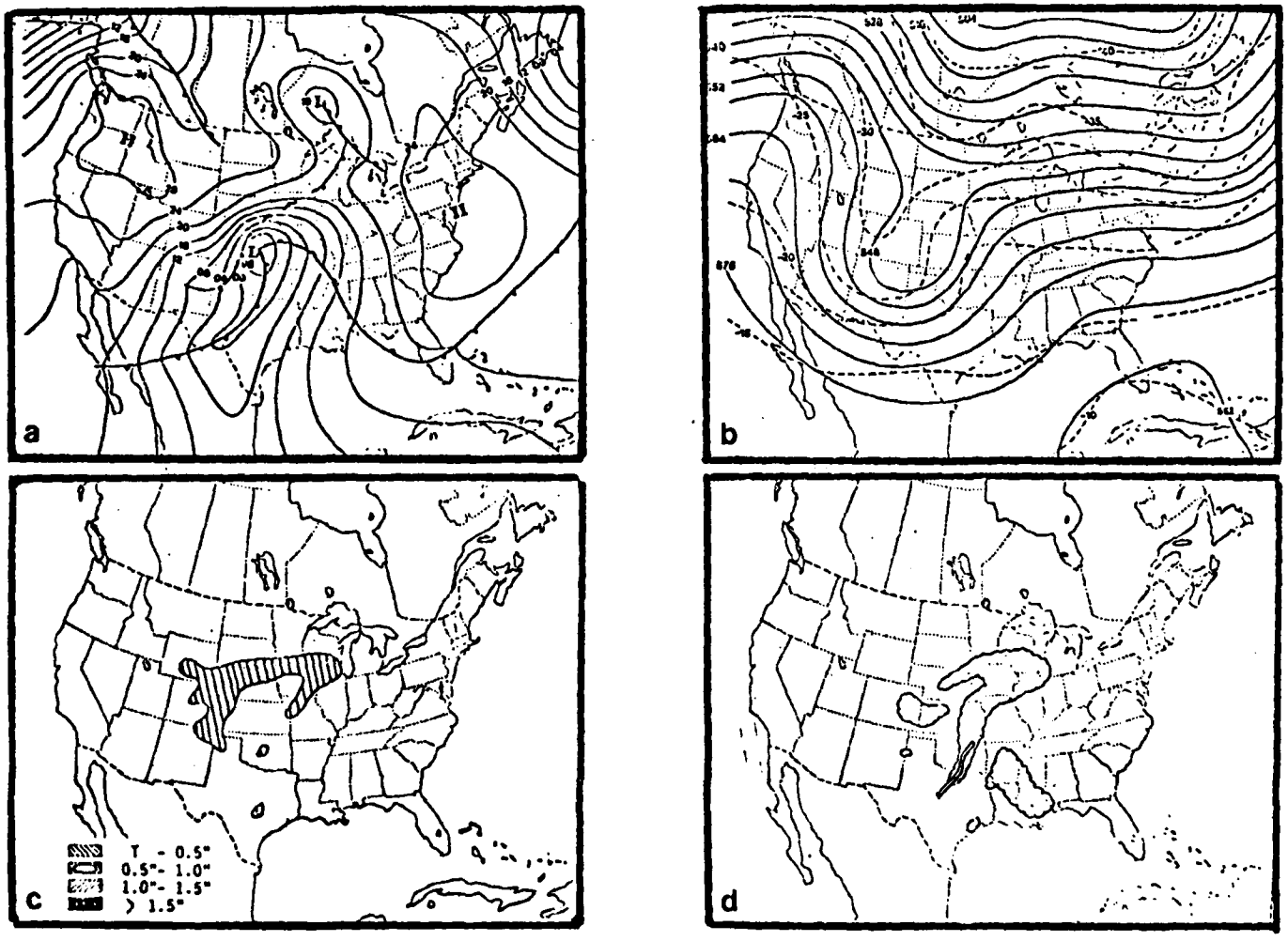

Figure 6. (a) Sea level pressure analysis, (b) 500 mb analysis, (c) 6 hour precipitation amounts, and (d) radar summary at 0000 GMT 21 February 1976.

precipitation had occurred (Fig. 6c and 6d). One area of precipitation was associated with moist air overrunning the warm front in Iowa. Another area was related to a line of thunderstorms with radar tops up to 45,000 feet ahead of the cold front in Nebraska and Texas. Although the area south of the surface low was very unstable, as depicted in the line of prefrontal thunderstorms (Fig. 7c) the moisture was confined to the prefrontal area while a large area west of the cold front was very dry at 850 and 500 mb as shown in Fig. 7a and 7b.

Synoptic Situation at 1200 GMT 21 February 1976

By the third map time, the surface low had moved into eastern Kansas with nearly no vertical tilt and where now one closed contour appeared at the 500 mb level (Fig. 8a and 8b). The cold front had moved rapidly eastward into northern Indiana and formed warm front type of occlusion that extended back to the cyclone center in eastern Kansas.

During the preceeding twelve hours the line of thunderstorms became more extensive along the cold front. Six hour precipitation accumulations amounted to 0.50 inches along the cold front and several stations reported amounts in excess of one inch (Fig. 8c and 8d). Satellite pictures showed a distinct dry tongue (a characteristic of occluding systems) forming between the cold front and the surface low in Kansas (Fig. 9c). Coincident with this dry tongue were the patterns of relative humidities which showed the dry tongue and the wrap around moisture surrounding the Kansas low (Fig. 9a and 9b).

Synoptic Situation at 0000 GMT 22 February 1976

By this fourth map time, the cyclone over Kansas filled by 4 mb

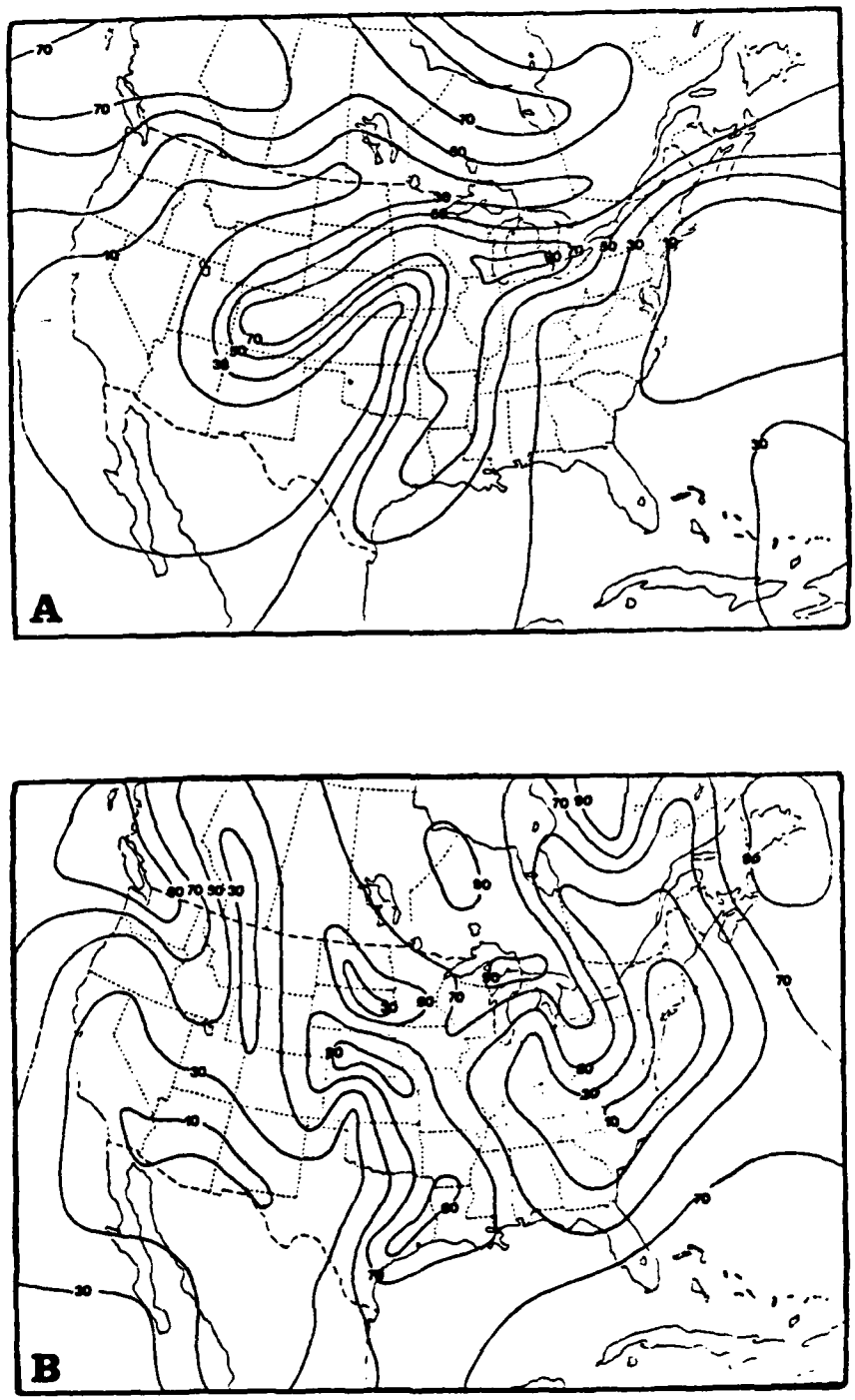

Figure 7. Relative humidity analysis at 0000 GMT 21 February 1976 for the (a) 500 mb level and (b) 850 mb level.

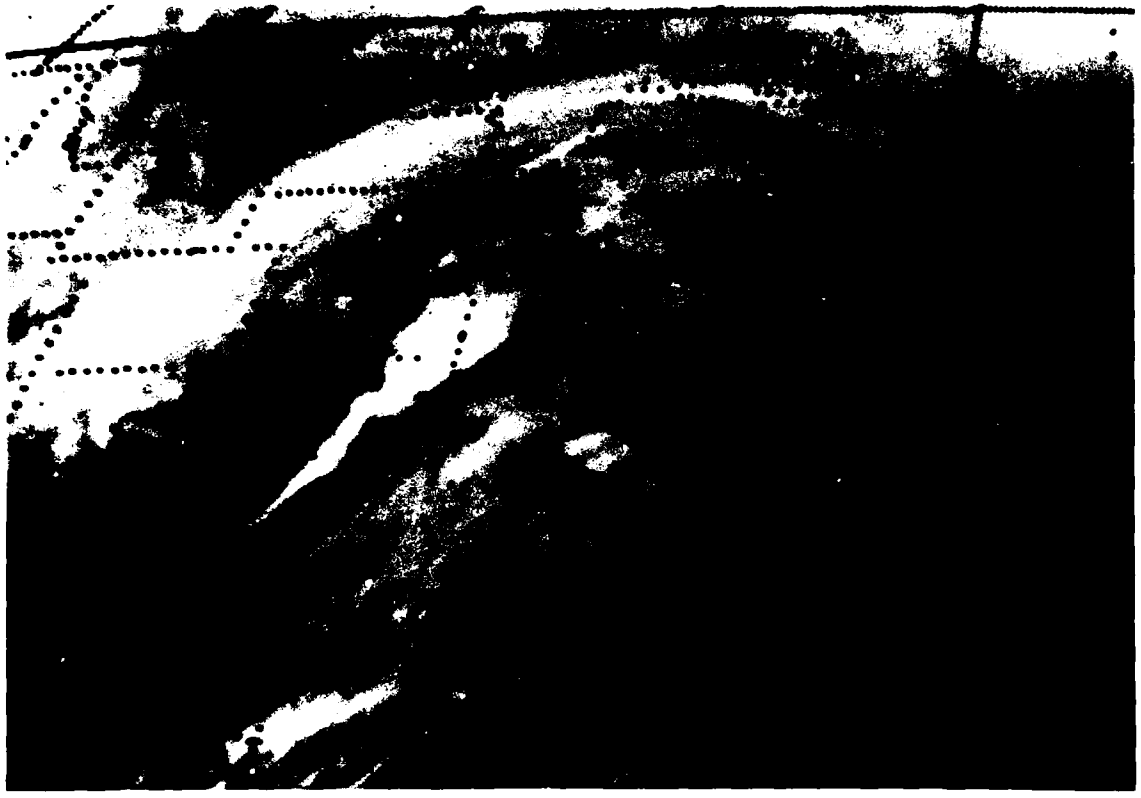

Figure 7. (c) GOES-East infrared satellite imagery at 0000 GMT 21 February 1976.

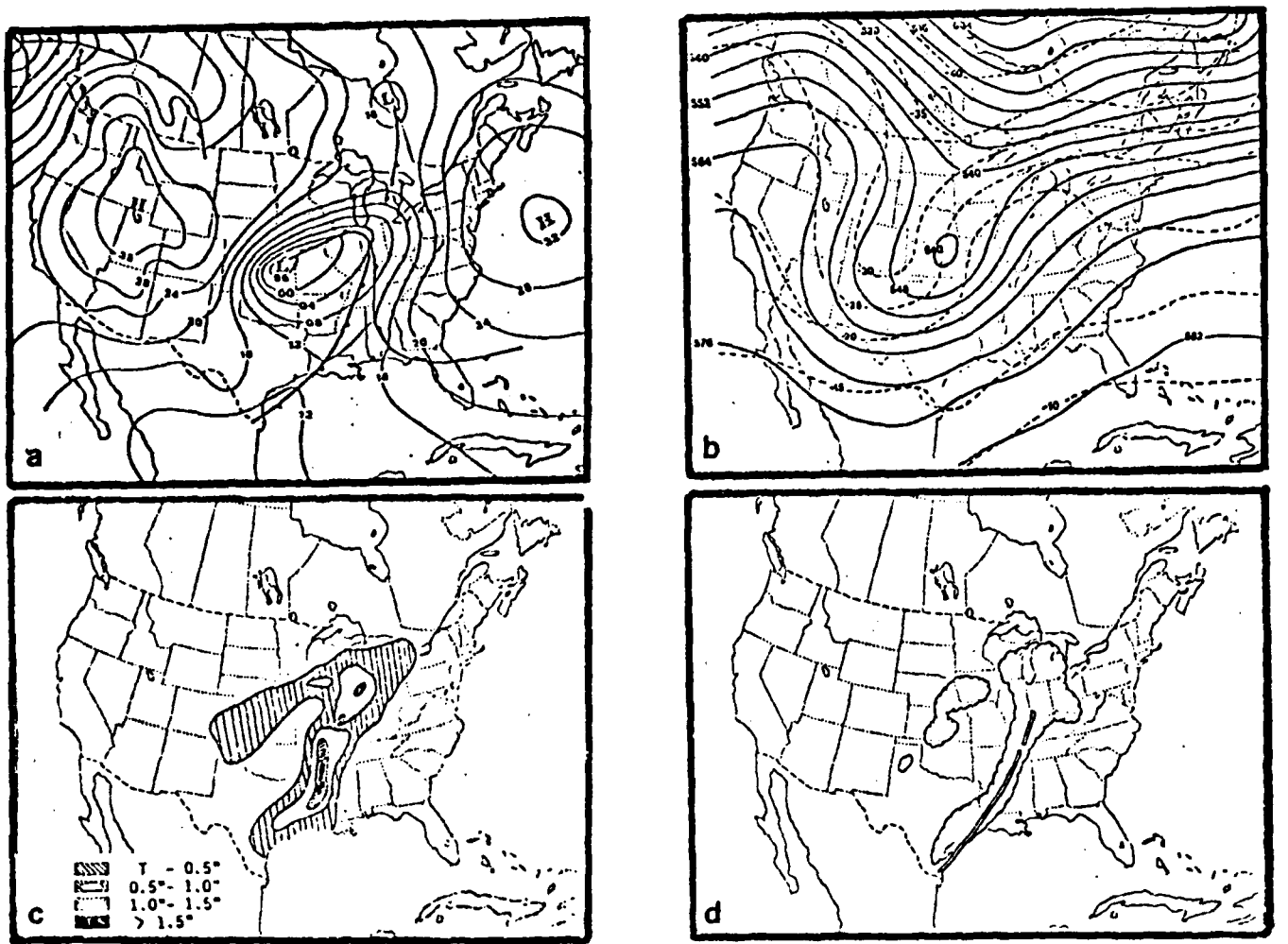

Figure 8. (a) Sea level pressure analysis, (b) 500 mb analysis, (c) 6 hour precipitation amounts, and (d) radar summary at 1200 GMT 21 February 1976.

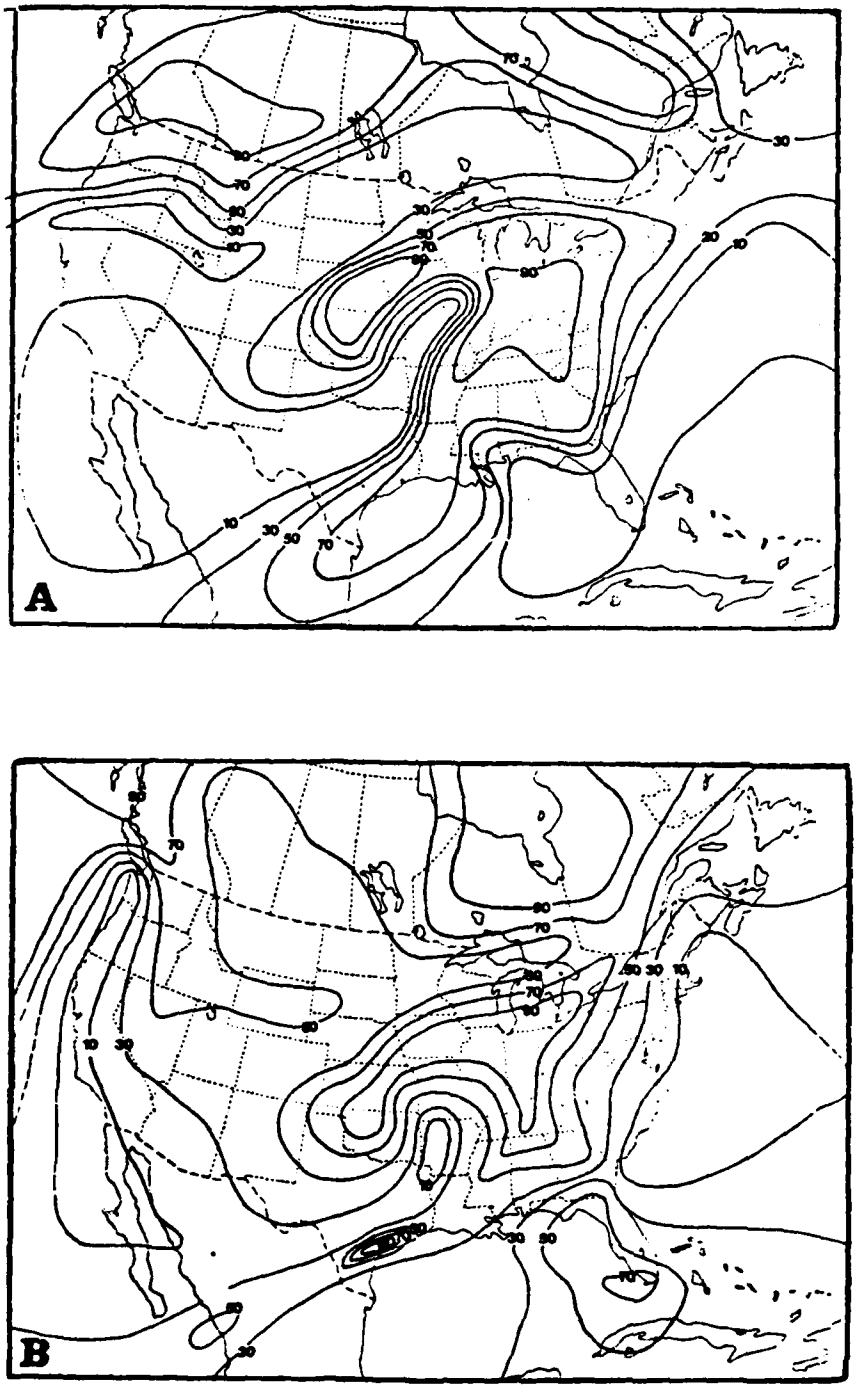

Figure 9. Relative humidity analysis at 1200 GMT 21 February 1976 for the (a) 500 mb level and (b) 850 mb level.

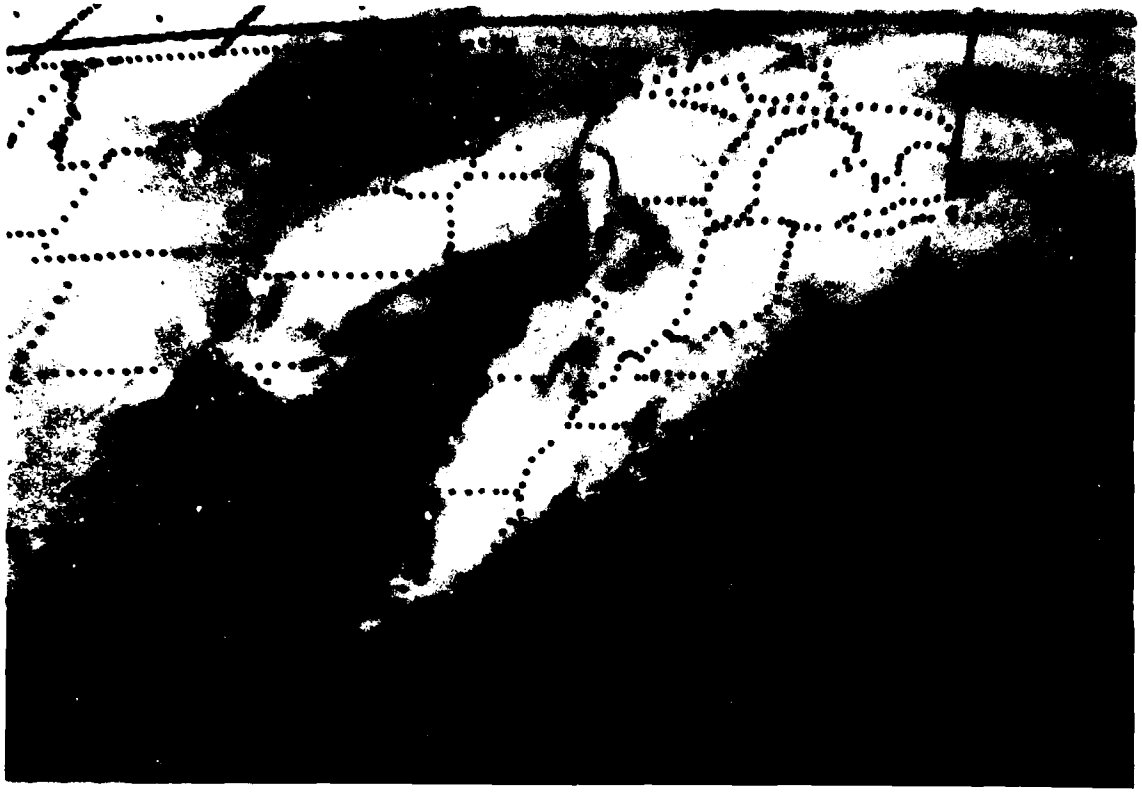

Figure 9. (c) GOFS-East infrared satellite imagery at 1200 GMT 21 February 1976.

from the previous 12 hours, while a second cyclone formed over Indiana (Fig. 10a). The surface pressure gradient weakened considerably around the entire storm and the lowest pressure was only 1004 mb. Also, there was a weakening of the 500 mb trough as the cold air advection diminished and as the trough began to fill (Fig. 10b).

Six hour precipitation amounts showed a corresponding decrease as the storm weakened (Fig. 10c and 10d). Moisture analyses showed abundant low level amounts throughout the entire area west of the Appalachian Mountains. The 500 mb relative humidities continued to exhibit a dry tongue behind the cold front which extended into central Michigan (Fig. 11a and 11b). The infrared satellite indicated two distinct cloud layers in the vicinity of the dissipating Kansas low and a cirrus shield along the cold front (Fig. 11c). The surface low system moved off the east coast of Maine by 0000 GMT 23 February. The 500 mb trough followed.

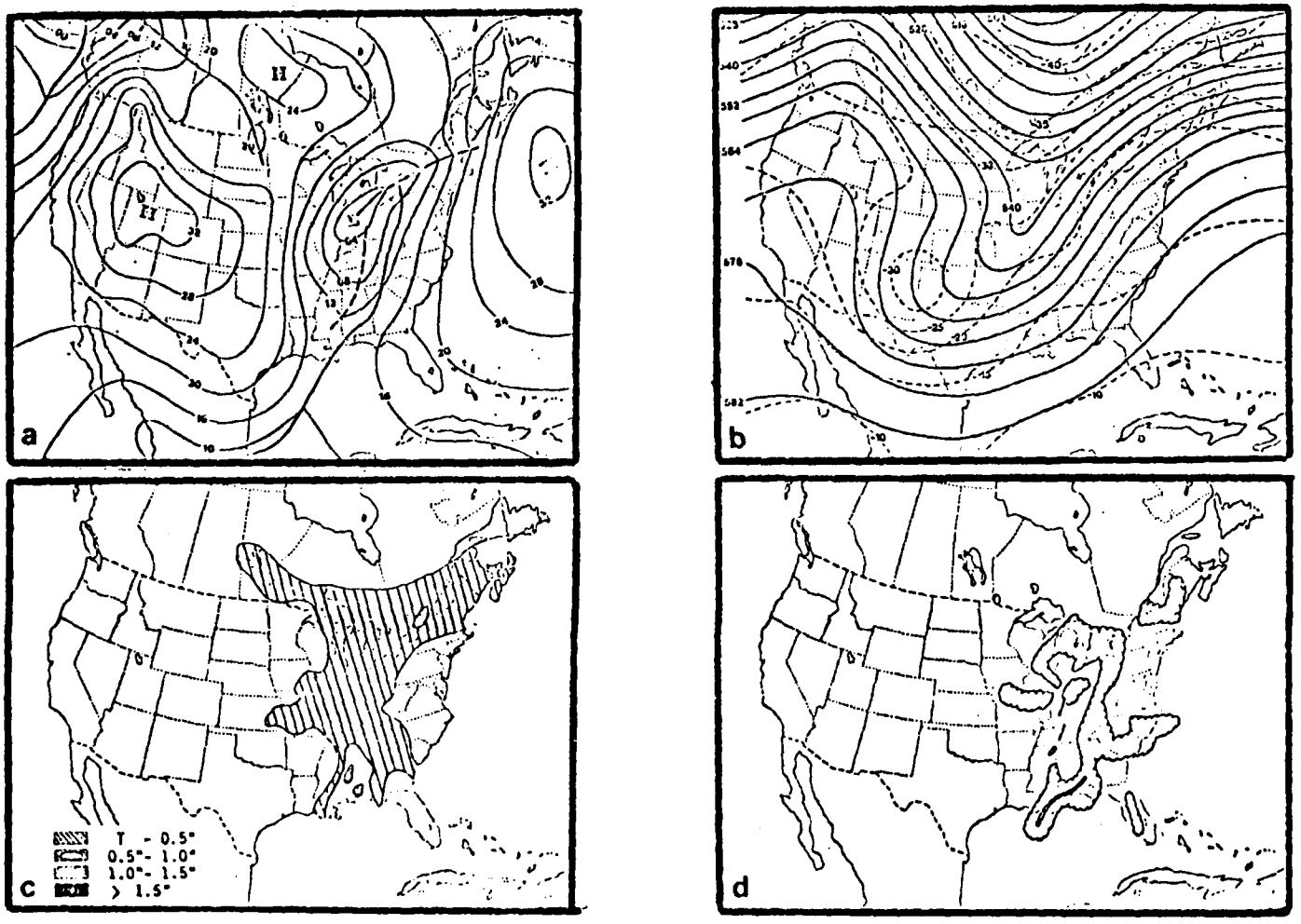

Figure 10. (a) Sea level pressure analysis, (b) 500 mb analysis, (c) 6 hour precipitation amounts, and (d) radar summary at 0000 GMT 22 February 1976.

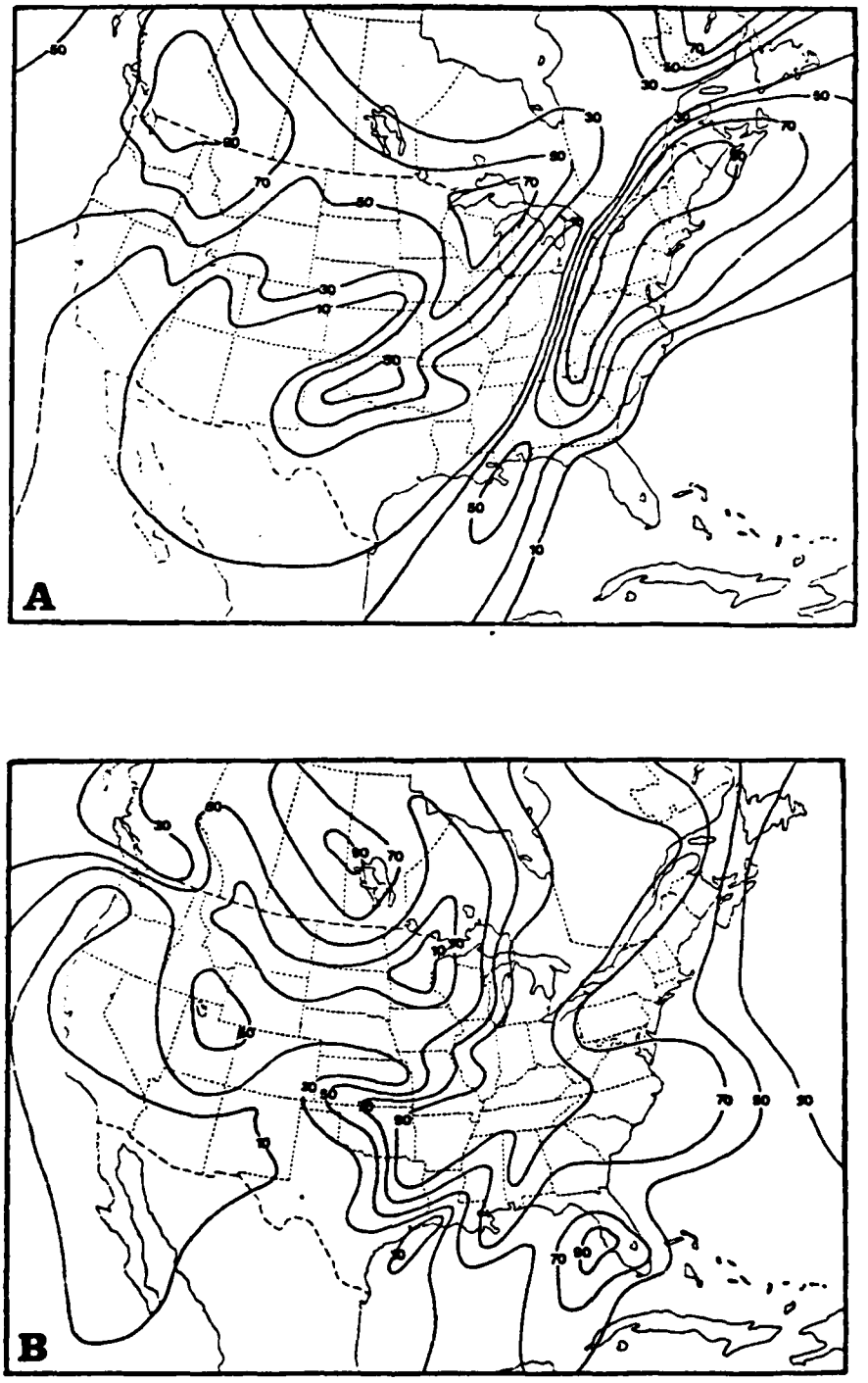

Figure 11. Relative humidity analysis at 0000 GMT 22 February 1976 for the (a) 500 mb level and (b) 850 mb level.

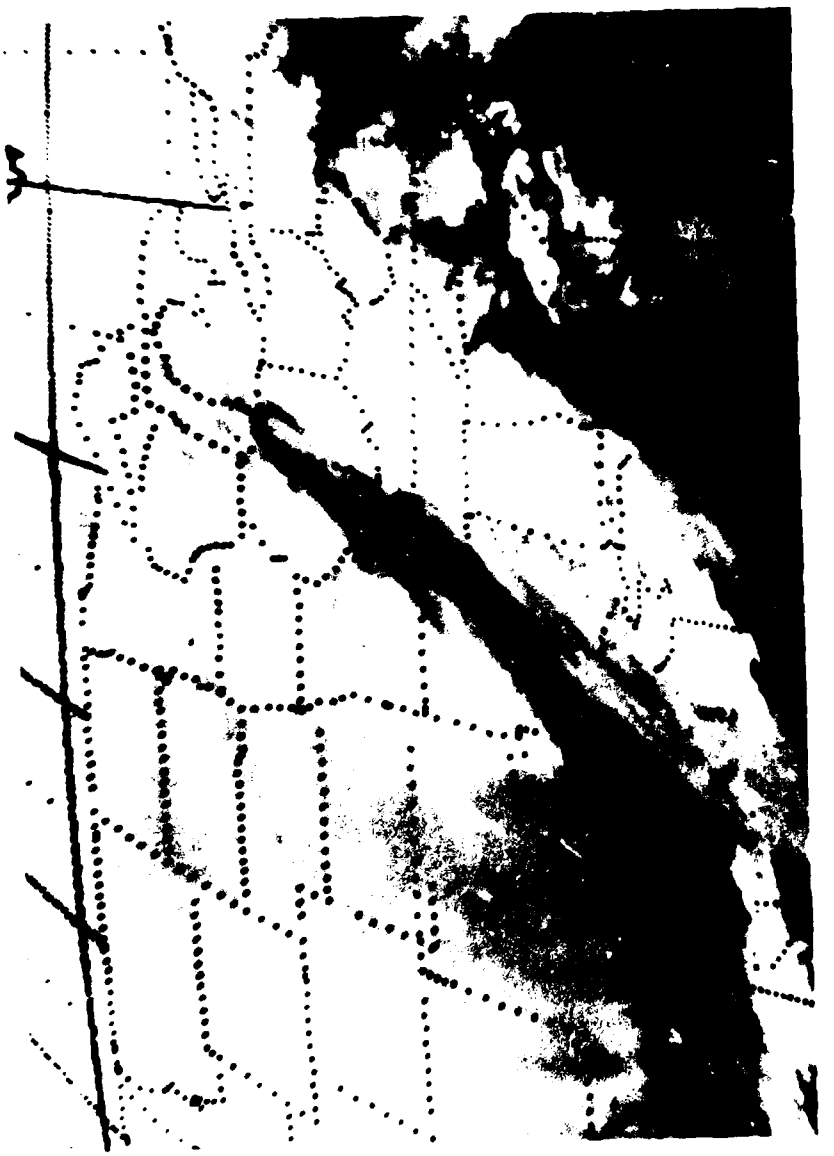

Figure 11. (c) GOES-East infrared satellite imagery at 0000 GMT 22 February 1976.

CHAPTER IV

COMPARISONS OF VERTICAL MOTION AND TEMPERATURE FIELDS WITH SYNOPTIC PATTERNS AND SATELLITE INFRARED RADIATION DATA

Vertical Motions

The detailed results of the numerical computations of the vertical motion fields for all four map times are depicted in Figs. 12-25. Comparions of the omega fields portrayed in the following figures showed good agreement with the synoptic patterns described in Chapter 3. In general, the omega value associated with this intense storm appeared to be very reasonable for a wintertime mid-latitude cyclone. Largest omega value ranged from +5 to -8 $\mu b\ s^{-1}$ and exhibited a typical cellular configuration with areas of ascent ahead of and subsidence behind the cyclone. Careful examination of the details in the vertical motion field revealed some interesting asymmetric features around the cyclone center and provided considerable insight into the role of the complex physical mechanisms involved during the storms evolution.

Three different graphical methods were used to display the vertical motions for each of the four synoptic map times. The total upward and downward motions for the 900, 700 and 500 mb surfaces trace the evolution of the storm from the initial stages of development through an intensification stage and finally through the occlusion stage all

within a 36 hour period. East-west vertical cross sections of the total omega along two different latitudes through the cyclone from 1000 to 100 mb are examined for vertical strengths within the troposphere. Finally, the vertical motions at the 900 mb and 500 mb surfaces are partioned in graphic form in order to display contributing forcing functions in a temporal wave phase propagation manner.

Development Stage - 1200 GMT at 20 February 1972

In general, the rising motions exhibited significant tilt with height from 900 to 500 mb. In Fig. 12, the cyclonic system in the lee of the Rockies is nearly vertical with the omega pattern at 900 mb and 700 mb almost identical in the Great Plains region. Although the zero isopleth for all three levels are coincident the location of the two centers of maximum values of omega at 500 mb indicate a northwestward tilt. From Fig. 3a and 3b, these displaced positions of maximum rising motion conform with the motions ahead of the surface and 500 mb low pressure centers.

A vertical cross section of omega values extending east-west through the upper level trough along 40°N latitude is shown in Fig. 13. A vertical core of -4 $\mu b\ s^{-1}$ ahead of the cyclone extended throughout the troposphere. This vertical cross section is slightly north of the -5 $\mu b\ s^{-1}$ centers in Fig. 12 and this vertical displacement indicates the 700 mb omega maximum is east of the lower level omega maximum, and the system should weaken in intensity. This vertical cross section in Fig. 13 includes the orographically induced vertical motions below 900 mb, while the total omega from Fig. 12 did not include this term.

From development to decay the storm was located between the Rocky

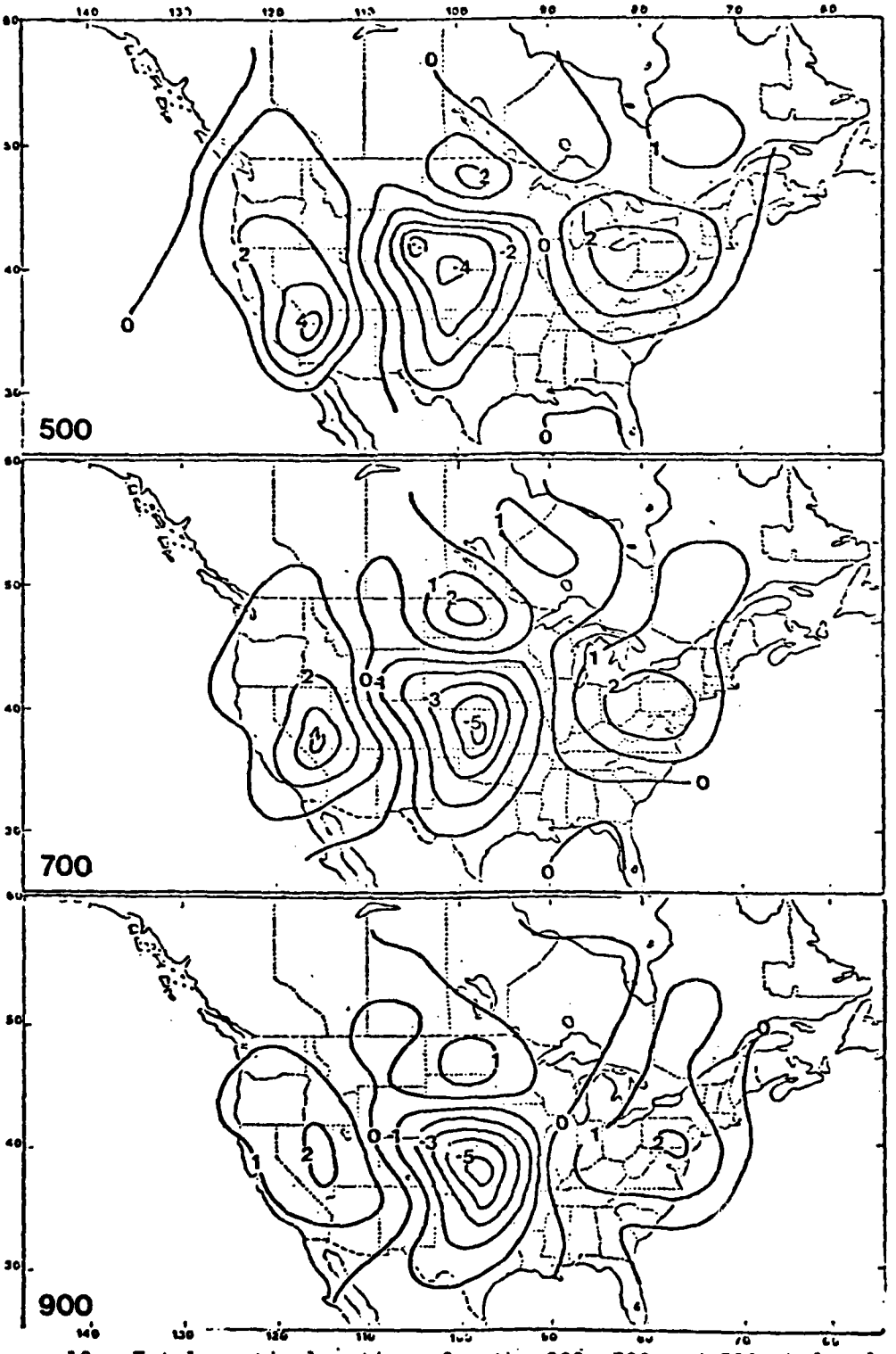

Figure 12. Total vertical motions for the 900, 700 and 500 mb levels at 1200 GMT 20 February 1976. Isopleth interval is 1 $\mu b\ s^{-1}$.

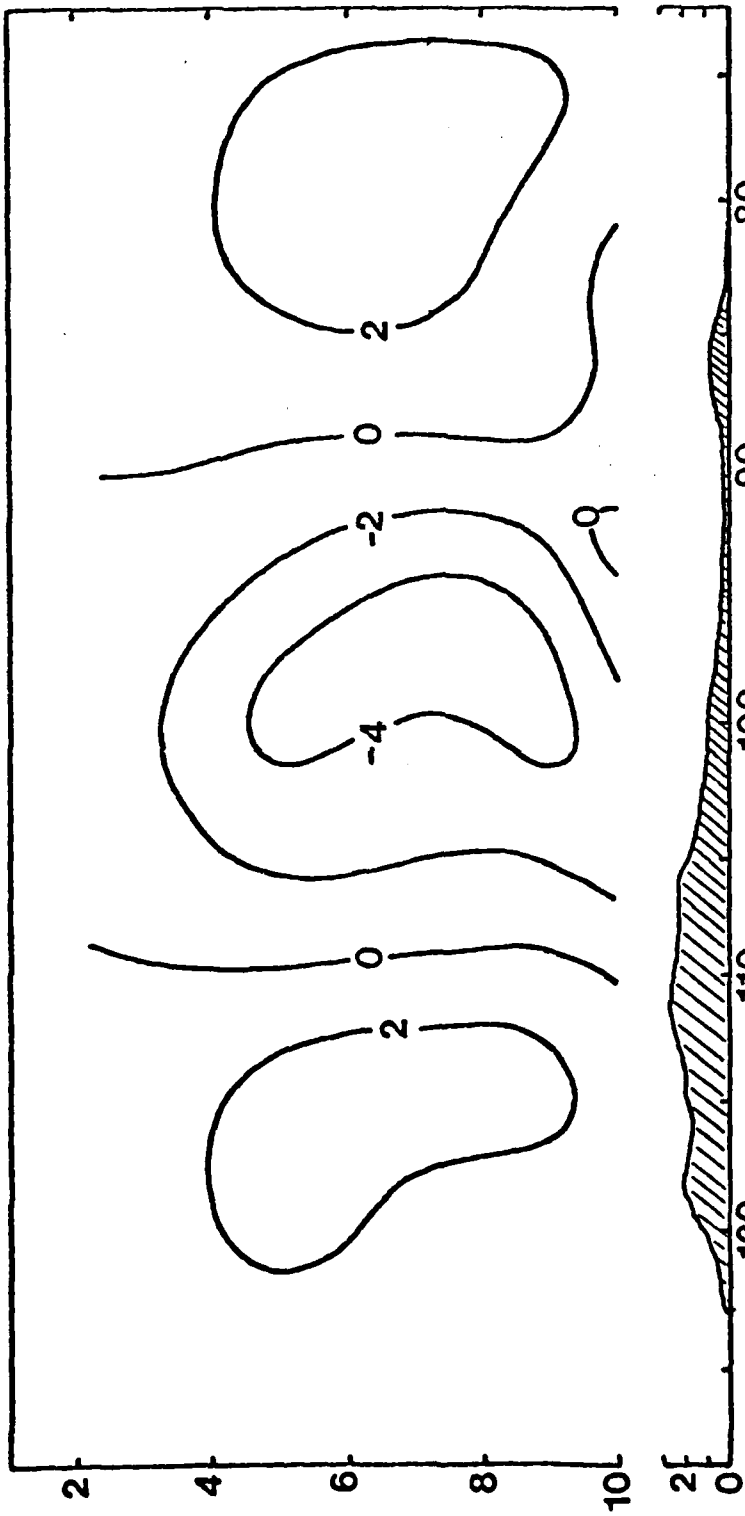

Figure 13. East-West cross-section of total vertical motions along 40°N latitude at 1200 GMT 20 February 1976. Isopleth interval is 2 μb s^{-1}. Ordinate units are 10^2 mb and 10^3 m.

and Appalacian mountain ranges with the second and third map times of 0000 GMT and 1200 GMT 21 February occurring in the relatively low level central United States. The (x,y,p) coordinate system is somewhat artificial near the lower boundary due to reduction of data to sea level, and this boundary is at best only a compromise for the actual upslope and downslope motion of air. Therefore, in the boundary layer only one omega level (900 mb) was used to compute vertical motion for pressure levels below 900 mb.

Contributions by each of the forcing functions defined in Eq. (5) provided information about the physical mechanisms at four pressure levels that can primarily be attributed to the ascending and descending motions through the storm evolution. Fig. 14 illustrates the east-west cross section of vertical motion contributions for the 900 mb and 500 mb surfaces. The cross section corresponds to the same 40°N latitude used in Fig. 13.

In each of the graphic representations of these omega contributions an insert is included to identify the location of the 500 mb trough and surface frontal systems relative to the cross section. The two horizontal lines coinciding with these pressure patterns indicate the 40°N and 37.5°N latitude lines from the 27 X 15 grid array, and the solid line represents the latitude line of the cross section. Partitioned omega values are displayed in the graphs only when their contribution was 10 percent or more of the upward and downward motions.

Examination of the various terms for all four map times resulted in determining the most significant contributors. Two terms dominated the 500 mb surface throughout the entire evolution period. These were differential vorticity advection by the nondivergent part of the wind

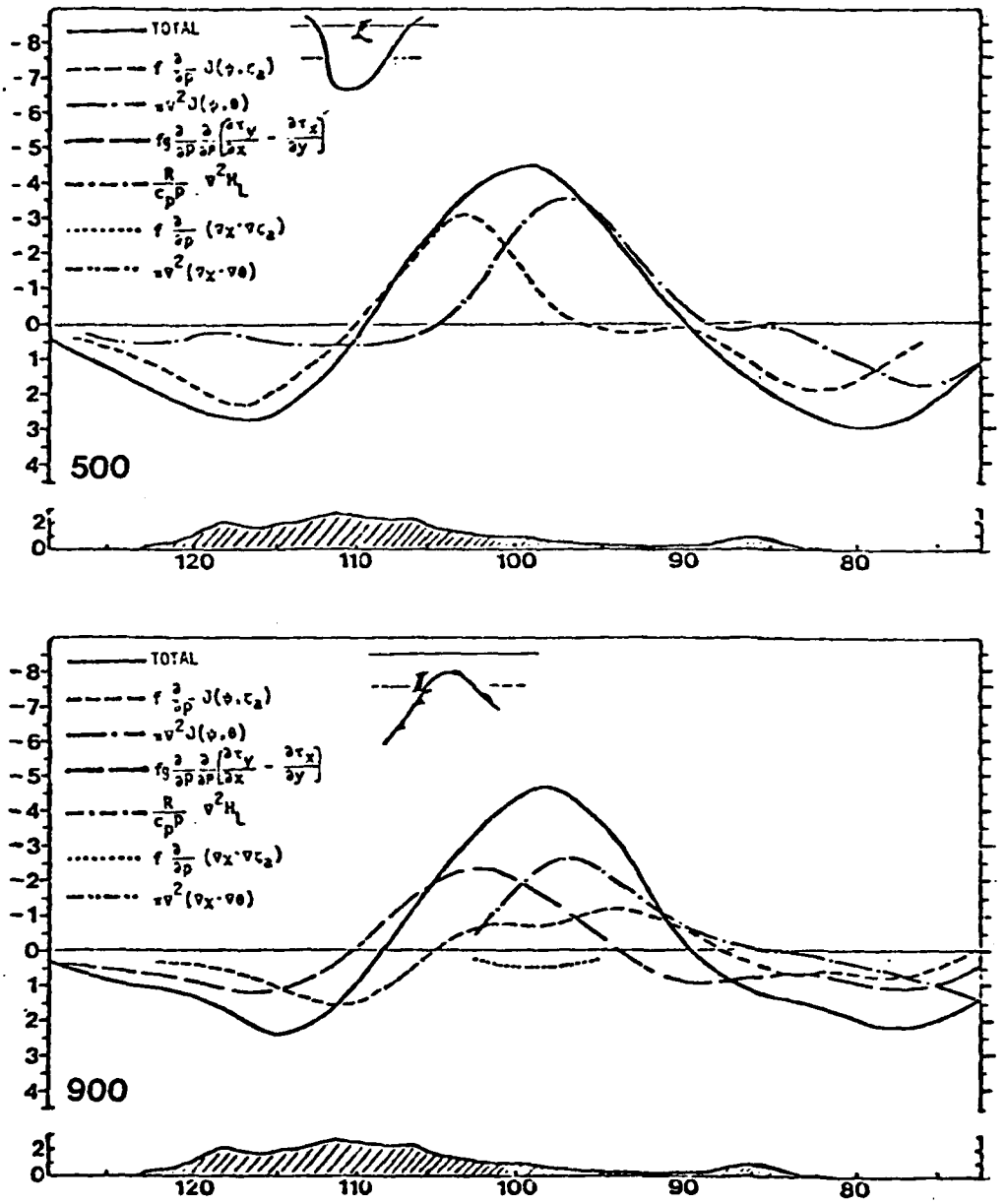

Figure 14. East-West cross-section of 900 and 500 mb partitioned vertical motions along 40°N latitude at 1200 GMT 20 February 1976. Ordinate units are 1 μb s^{-1} and 10^3 m.

and the Laplacian of thermal advection by the nondivergent part of the wind. The thermal effect was always east of the vorticity effect throughout the four map times, but they were always close enough in phase to contribute at least 85 percent to the maximum rising motions east of the storm center. Their individual contributions varied depending on the stage of the storm. Friction was the dominant term in all stages of the storm evolution at the 900 mb level, with various combinations of other forcing functions contributing at different periods for significant developments.

From Fig. 14 the differential vorticity advection and Laplacian thermal advection terms contributed over 90 percent at the 500 mb level. The subsidence region west of the upper air trough was primarily caused by the advection of negative vorticity, and only a minimum of cold air advection. In the lee of the Rockies positive vorticity advection initiated rising motion of $-3\ \mu b\ s^{-1}$ and the warm air advection wave which is east of the vorticity advection wave also contributed $-3\ \mu b\ s^{-1}$ of vertical motion.

The frictional stresses at the surface were the primary mechanism of low level upward and downward motion. Warm air advection and positive vorticity advection were both nearly in phase but trailed the frictional wave and contribute to the maintanence of the upward motion.

Intensification Period - 0000 GMT at 21 February 1976

For the second map time, the total vertical motion fields displayed an asymetric omega center at 900 and 700 mb in Fig. 15. The low level vertical motion of $-8\ \mu b\ s^{-1}$ was the largest value of ascending motion that was computed for the entire storm evolution. It

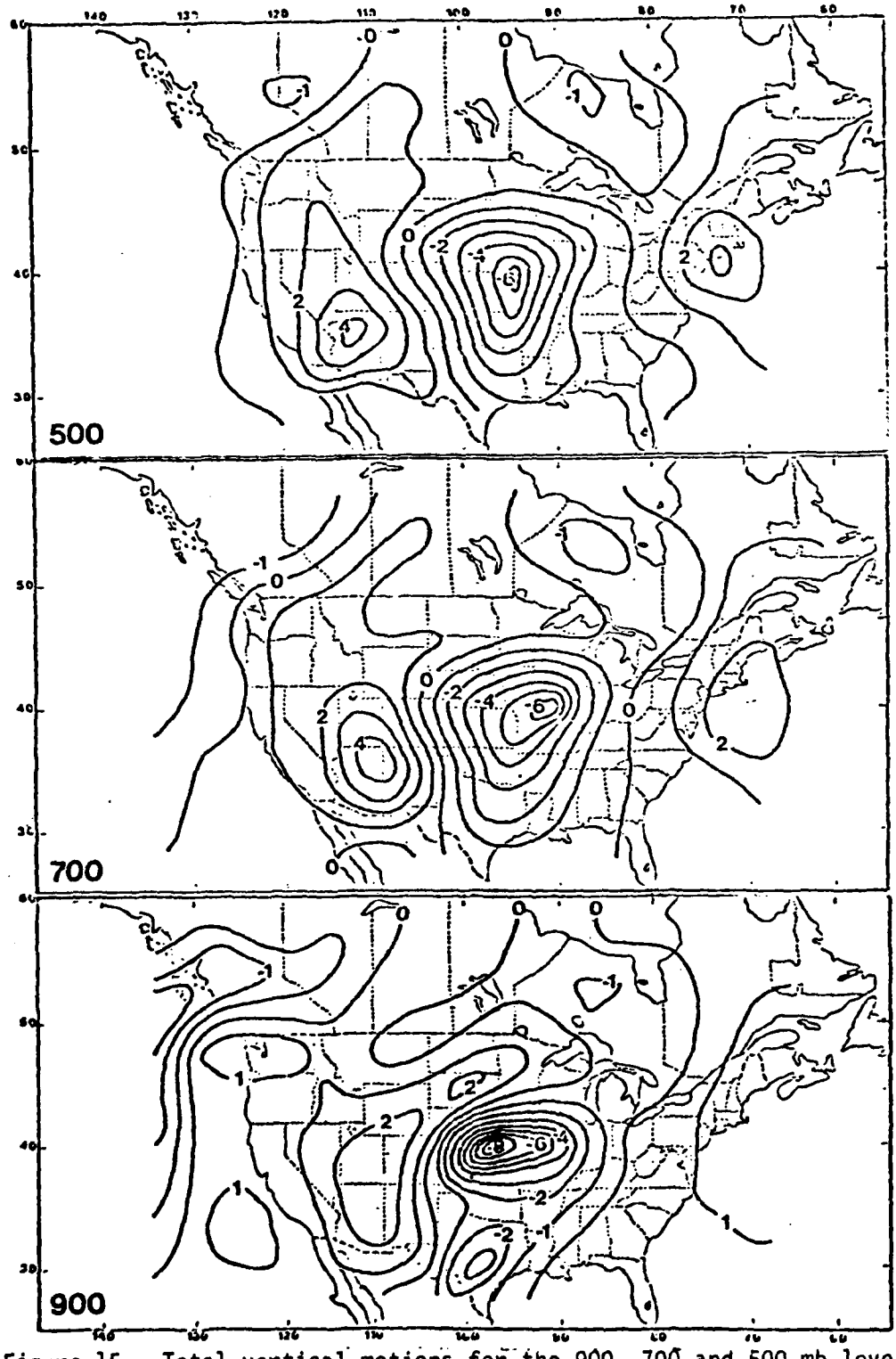

Figure 15. Total vertical motions for the 900, 700 and 500 mb levels at 0000 GMT 21 February 1976. Isopleth interval is 1 $\mu b\ s^{-1}$.

corresponded with the strongest pressure gradients around the surface low that was shown in Fig. 6a and also with the center of maximum storm development that was apparent in the enhanced satellite imagery in Fig. 30. The asymetric omega maximum of -6 $\mu b\ s^{-1}$, that extended eastward into Missouri at both 900 and 700 mb, corresponded to the position of the surface occlusion which developed in the following 12 hours. At 500 mb the maximum of -6 $\mu b\ s^{-1}$ tilted east with respect to the -8 $\mu b\ s^{-1}$ value at 900 mb and suggested the strong low level upward motion in Kansas would rapidly decay, while the -6 $\mu b\ s^{-1}$ 900 mb omega center would determine the new low pressure position.

The zero isopleth of vertical motion in Fig. 15 sloped upward toward the north from the 900 mb level to 500 mb. In South Dakota, low level subsidence was evident with upper level rising motion above it. The northern boundary of low level rising motion corresponded very closely with the northern edge of the echo pattern shown on the radar summary in Fig. 6c over South Dakota and Minnesota. The zero isopleth at all three levels also formed the western boundary of the echo pattern in Colorado.

Fig. 16 depicts the east-west tropospheric cross section at 40°N and illustrates the vertical extent of the upward motions. The intense core of -8 $\mu b\ s^{-1}$ slightly northeast of the surface low is evidently west of the -6 $\mu b\ s^{-1}$ core at 500 mb. This again would indicate that the western low level omega core was not very deep and would more likely be short-lived compared to the deeper layer of ascending motions near 92°W longitude.

The orographically induced rising motions (-4 $\mu b\ s^{-1}$) in the lee of the Rockies are also depicted very well in Fig. 16. The surface

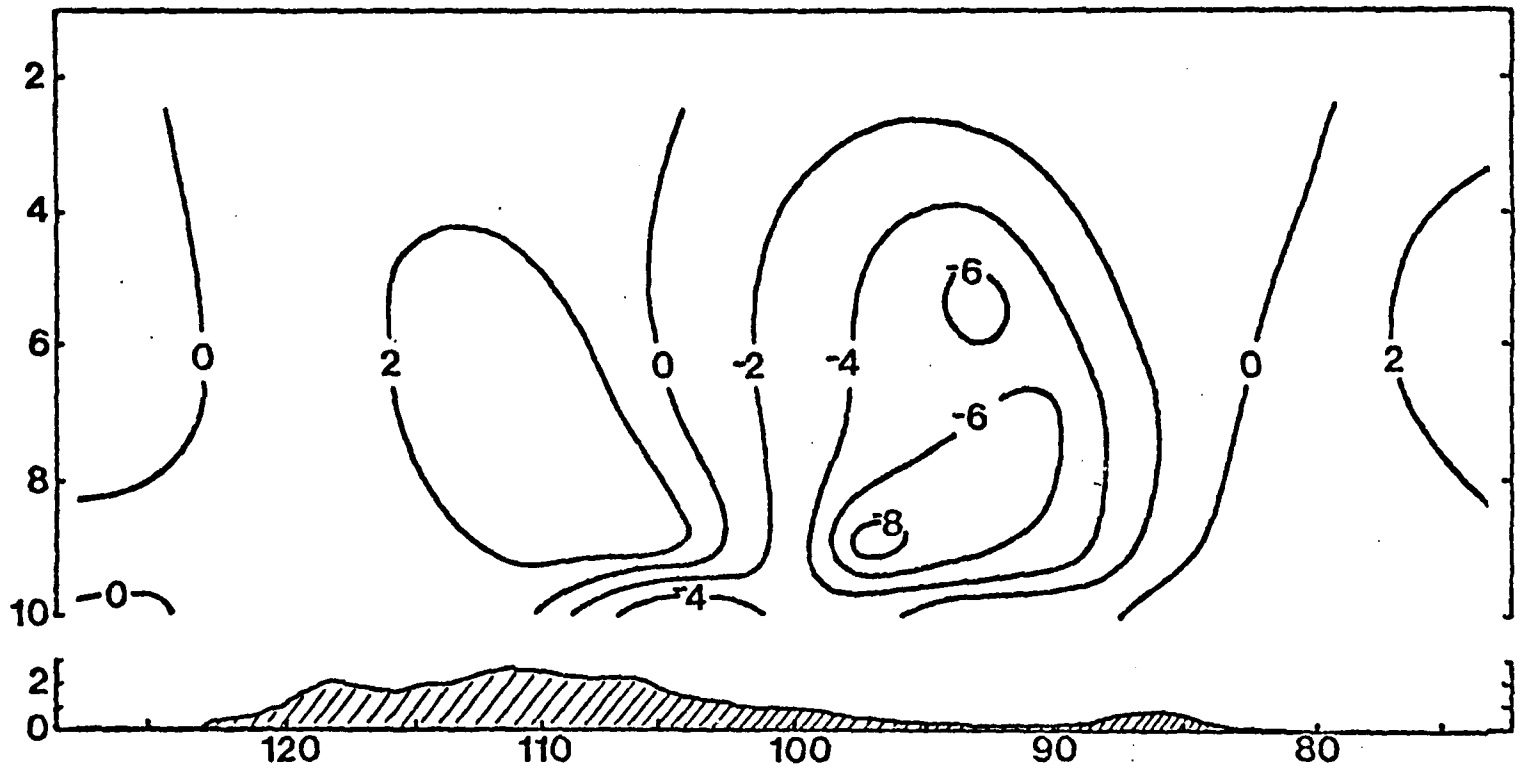

Figure 16. East-West cross-section of total vertical motions along 40°N latitude at 0000 GMT 21 February 1976. Isopleth interval is 2 $\mu b\ s^{-1}$. Ordinate units are 10^2 mb and 10^3 m.

low is centered between the -4 μb s^{-1} and -8 μb s^{-1} cores and the easterly component into the mountain at low level provides the lift for the small active area of showers on the Colorado and Kansas border (Fig. 6c).

The portioned omegas at the 500 mb level in Fig. 17 were typical of the developmental stage, with the addition of frictional stresses which were very strong at the surface (-6 μb s^{-1}) and contribute more than 10% to the total omega at higher levels. The vorticity advection wave due to the non-divergent part of the wind still leads the Laplacian of thermal advection wave by the non-divergent part of the wind although the thermal contribution of -4 μb s^{-1} exceeds the vorticity contribution of -3 μb s^{-1}. This thermal effect of increased warm air advection ahead of the 500 mb trough caused a deepening at the 500 mb surface as the thermal trough still lagged the pressure trough.

The 900 mb omega cross section illustrates the asymetric pattern from Fig. 15 together with the contributing partitioned omegas. The increased cyclone curvature around the strong surface low (Fig. 6a) were represented with the large friction contribution of -6 μb s^{-1}. This term decrease with increasing distance from the low pressure center and did not effect the secondary maximum at 88°W. The differential vorticity advection due to the divergent part of the wind was initially an important factor to the rising motions while further downstream this term produced descending motion. The thermal effect of low level warm air advection northeast of the low was now ahead of and stronger than the vorticity effect due to the non-divergent wind (-3 μb s^{-1} vs. -2 μb s^{-1}). The thermal term contributes almost 60% of the total eastward extension of vertical motion at 88°W.

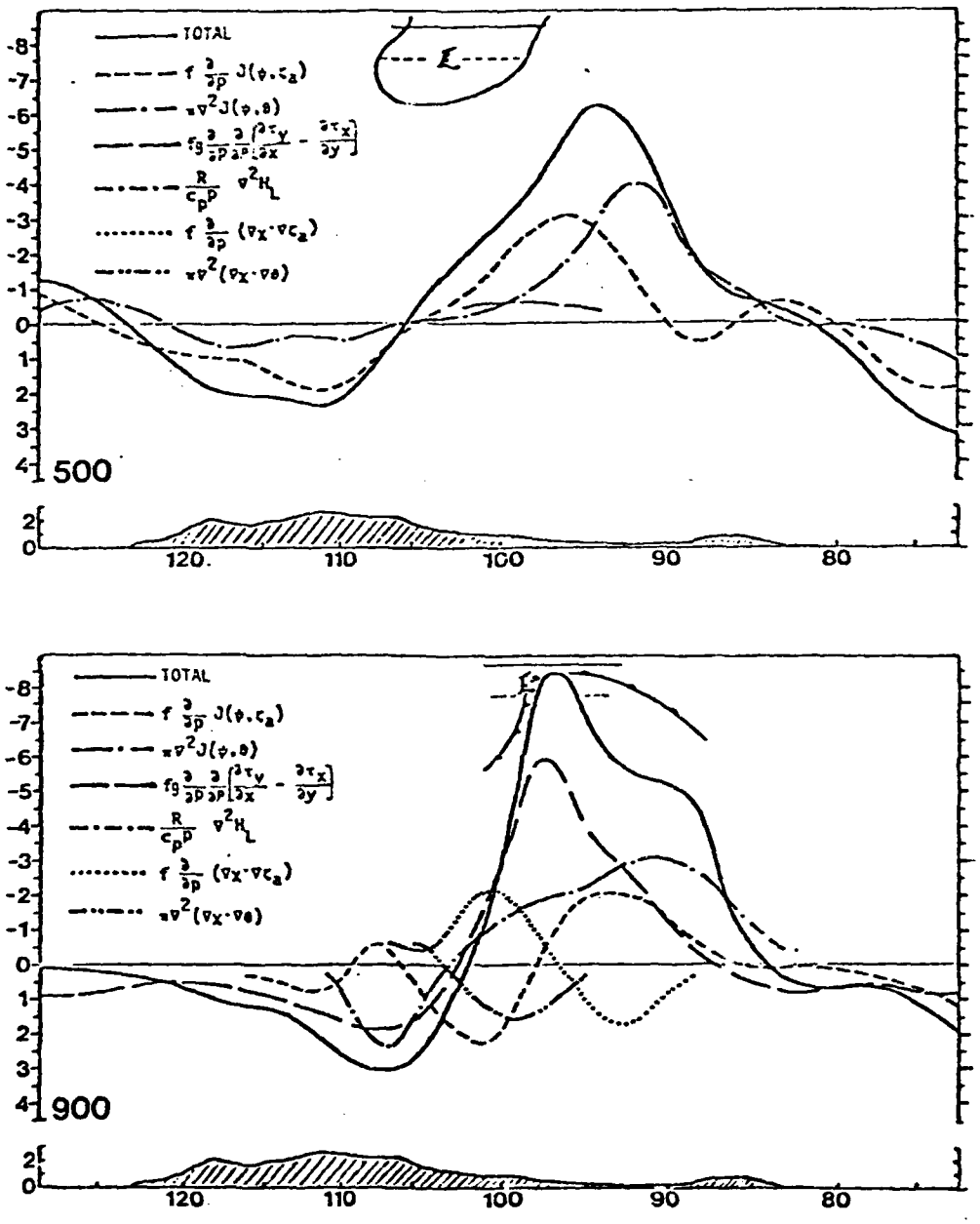

Figure 17. East-West cross-section of 900 and 500 mb partitioned vertical motions along 40°N latitude at 0000 GMT 21 February 1976. Ordinate units are 1 μb s^{-1}.

First Occlusion Stage - 1200 GMT at 21 February 1976

Fig. 18 displays two interesting areas of rising and sinking motion on the three horizontal planes at 900, 700 and 500 mb. At 900 mb the elongated asymetric omega pattern clearly defined the decaying Kansas low pressure center (Fig. 8a) with a -4 $\mu b\ s^{-1}$ core; the occlusion; and the triple frontal point over Indiana with -6 $\mu b\ s^{-1}$ of rising motion. A wedge of sinking motion at 900 mb spiraled into the dry tongue from a core of maximum downward motion of 5 $\mu b\ s^{-1}$ over southern Oklahoma. This wedge was an important factor in determing the northern extent of the dry tongue and the southern extent of the precipitation area (Fig. 8c) over Kansas. This subsidence tongue was visible to a lesser extent on the 700 and 500 mb levels (Fig. 18) as well as the relative humidity charts (Figs. 9a and 9b).

At this time the vertical tilt of the system from the 900 mb -6 $\mu b\ s^{-1}$ maximum to 500 mb was slightly westward for the first time in the evolution of the storm (Fig. 19). This tilt suggested that the system had not reached its peak, even though the total vertical motion at all levels for this map time were less than the previous map time when the severe weather occurred. From radar and precipitation summaries, the thunderstorm line and associated rainfall rates did increase substantially (Fig. 8c and 8d).

Fig. 19 also indicates a decrease in the vertical motions around the Kansas low pressure with only a -4 $\mu b\ s^{-1}$ core at 93°W latitude and an associated change in the easterly wind induced orographic upslope motion that decreased to -2 $\mu b\ s^{-1}$.

Both cross sectional levels at 500 and 900 mb from Fig. 20

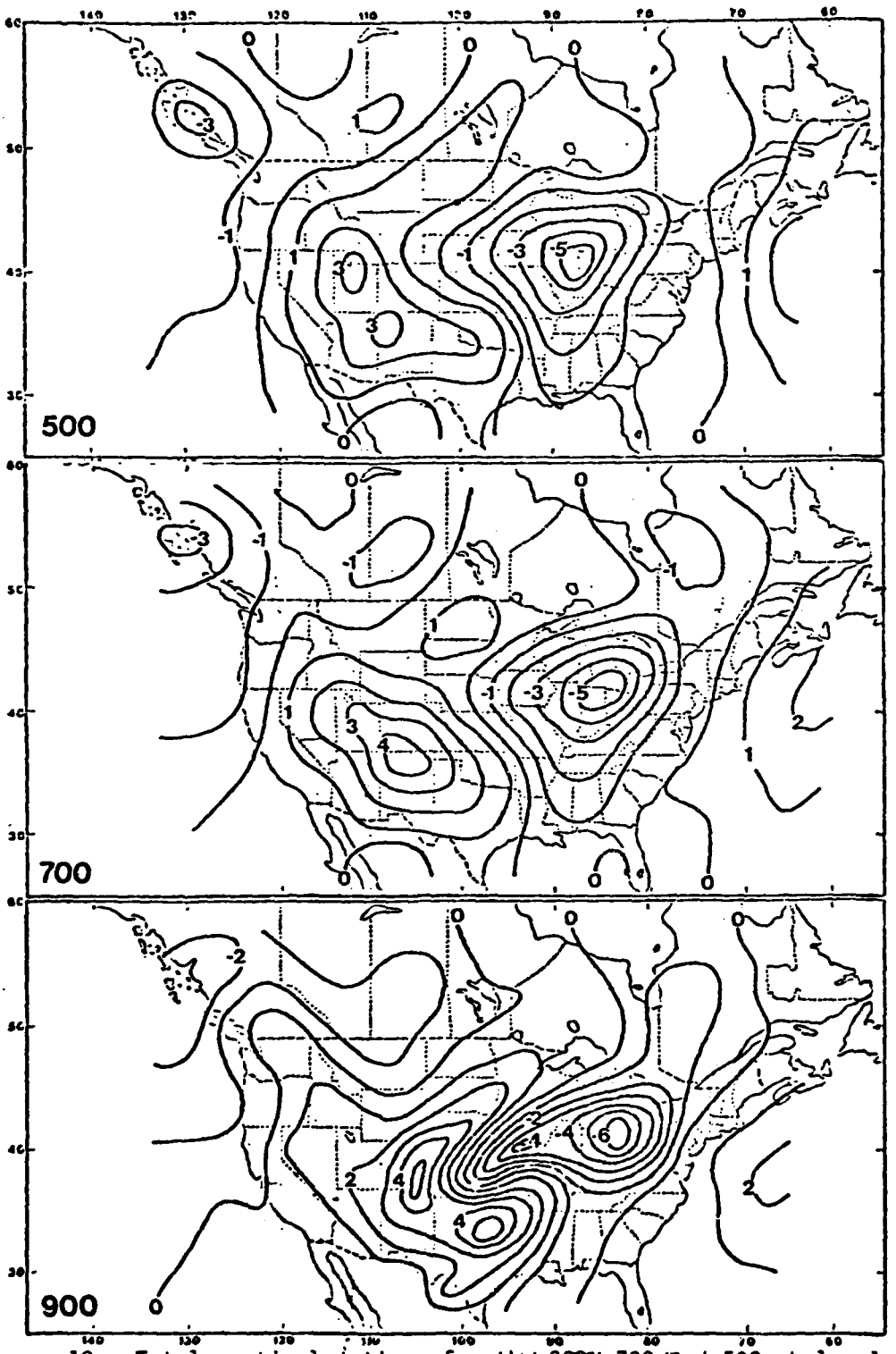

Figure 18. Total vertical motions for the 900, 700 and 500 mb levels at 1200 FMT 21 February 1976. Isopleth interval is 1 $\mu b\ s^{-1}$.

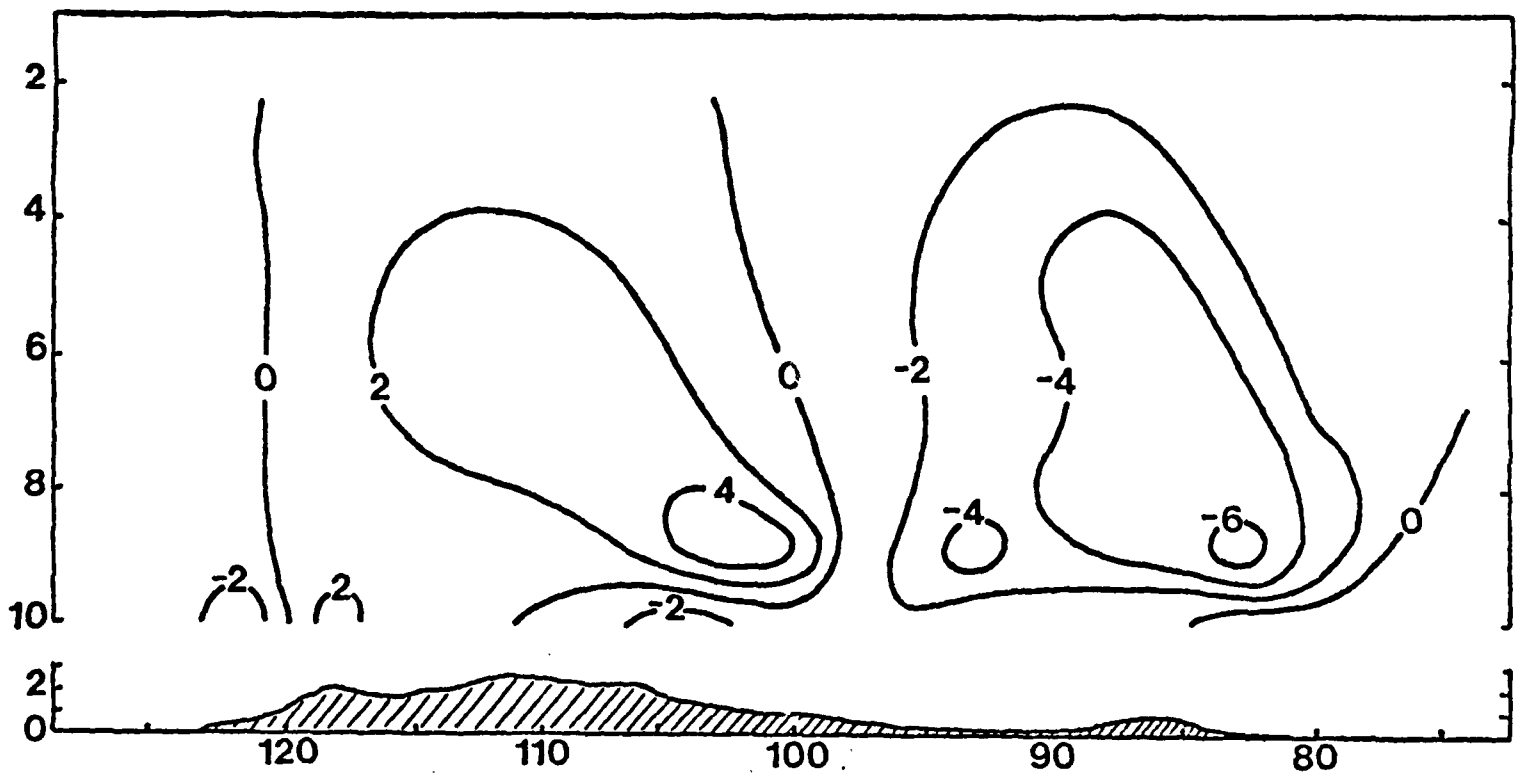

Figure 19. East-West cross-section of total vertical motions along 40°N latitude at 1200 GMT 21 February 1976. Isopleth interval is 2 μb s^{-1}. Ordinate units are 10^2 mb and 10^3 m.

provided information to diagnose the synoptic development. The thermal trough at the 500 mb level continue to lag the pressure trough. This was evident in the phase displacement of vorticity and thermal advection although there was a decrease in the warm air advection ahead of the pressure trough and an associated decrease in vertical motions induced by the thermal advection (2.5 $\mu b\ s^{-1}$).

Also, by this time, the prefrontal thunderstorm activity indicated a contribution from latent heat release from the convection over the Appalacians. This convective activity was not as rapid in formation as the severe weather from the Kansas low but it encompassed a larger area that was located in Indiana and Illinois.

The decay of the Kansas low and development of the Indiana low was clearly evident on the 900 mb cross section of Fig. 20. The circulation around the decaying low was still intense enough to produce -6 $\mu b\ s^{-1}$ of rising motion due to frictional effects. The total omega however was only -5 $\mu b\ s^{-1}$ due to the strong downward motion contribution from vorticity advection by the divergent part of the wind. As the 500 mb closed low became almost vertical with the Kansas low, this contribution reached a maximum and caused the low to fill as expected. Vorticity and thermal effects from the non-divergent wind were generally small as the phase difference became more pronounced and these two terms tended to cancel each other around the Kansas low. Their total contribution of 3.0 $\mu b\ s^{-1}$ did provide energy for the maintenance of the Indiana low, however.

Figs. 21 and 22 also depict cross sections for the third map time of 1200 GMT 21 February 1976. In order to provide a better explanation of the dry tongue a cross section was also included for

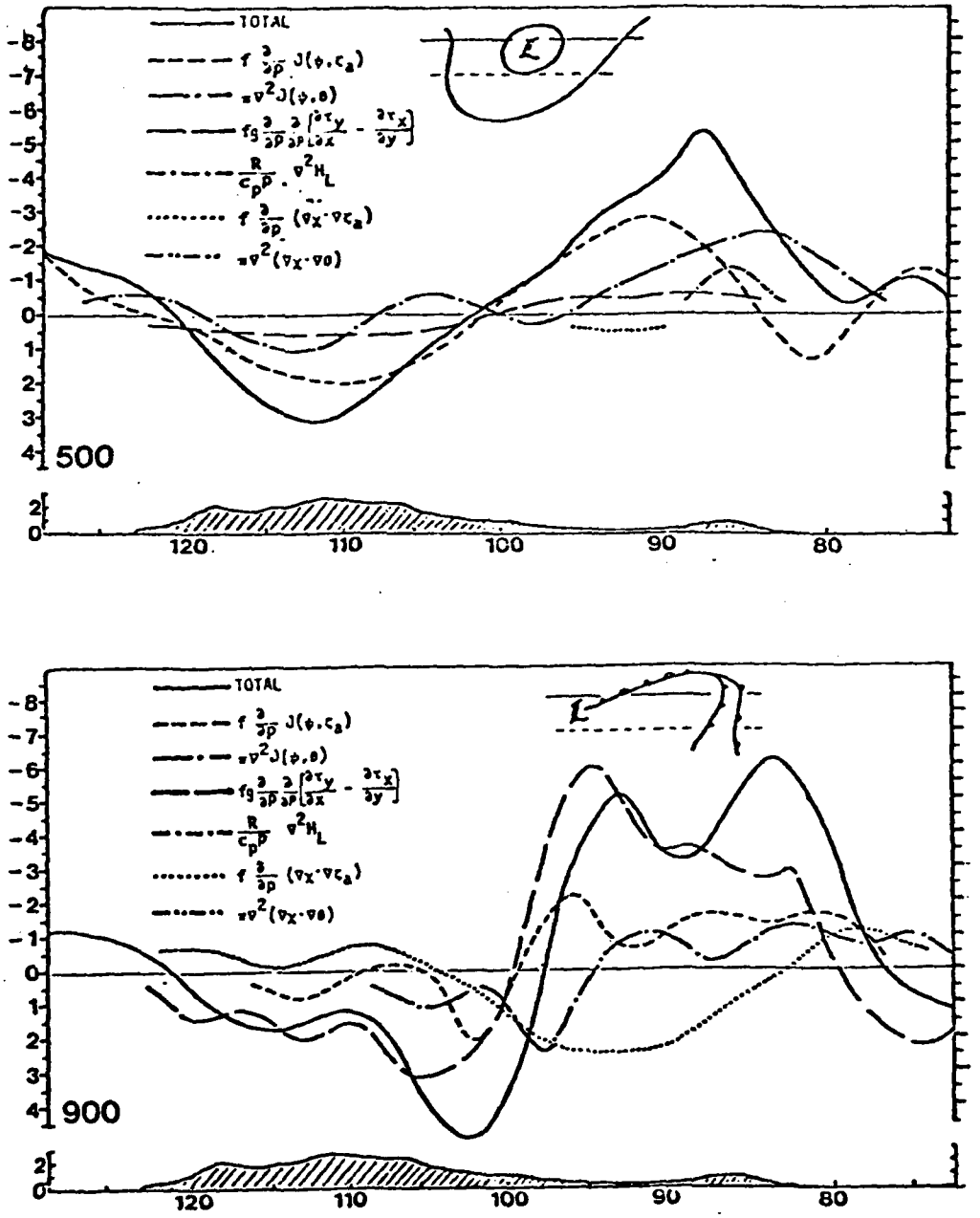

Figure 20. East-West cross-section of 900 and 500 mb partitioned vertical motions along 40°N latitude at 1200 GMT 21 February 1976. Ordinate units are 1 μb s^{-1} and 10^3 m.

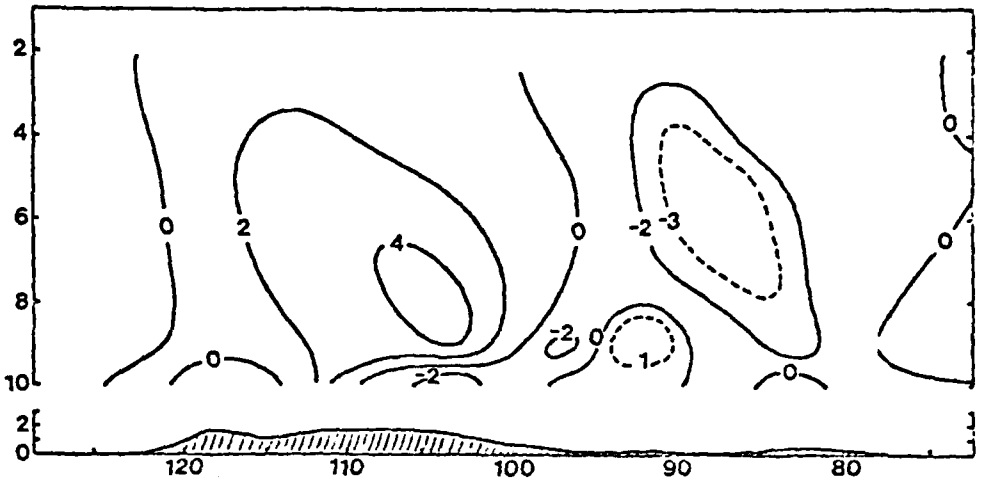

Figure 21. East-West cross-section of total vertical motions along 37.5°N latitude at 1200 GMT 21 February 1976. Isopleth interval is 2 μb s^{-1}. Ordinate units are 10^2 mb and 10^3 m.

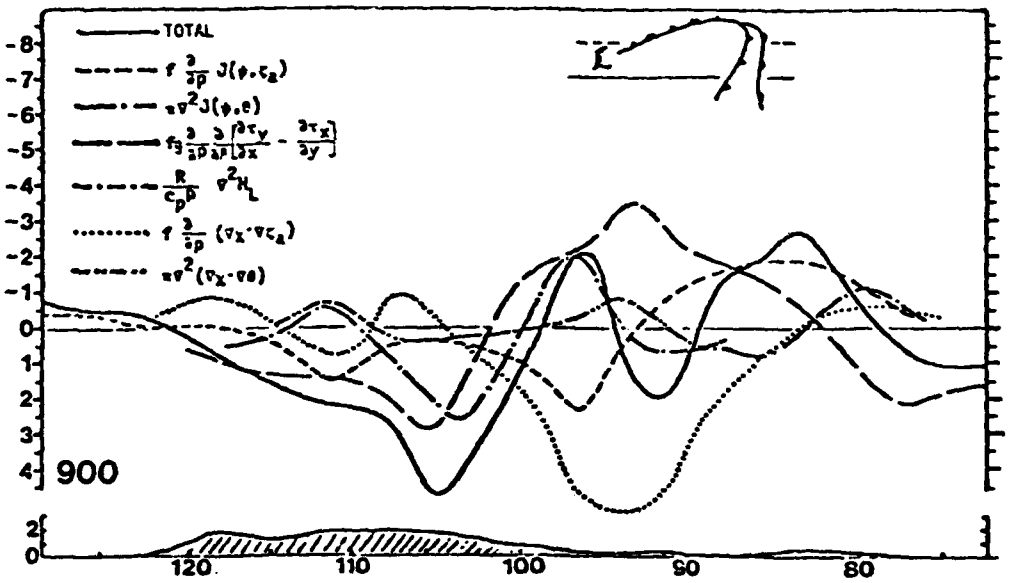

Figure 22. East-West cross-section of 900 mb partitioned vertical motions along 37.5°N latitude at 1200 GMT 21 February 1976. Ordinate units are 1 μb^{-1} and 10^3 m.

37.5°N latitude. From Fig. 21 the vertical depiction from 1000 to 100 mb accurately position the dry tongue subsidence area between the cold front and the Kansas low. An interesting feature is the shallow extent of the area of descending motion. The omega values increased with a zero field at 800 mb. From the relative humidity chart the air at 500 mb was dry enough to retard clouds and maintain the dry tongue (Figs. 9a and 9b) even in an area of rising motions.

The contributions to this subsidence area are graphically displayed in Fig. 22. Frictional effects on the southern side of the Kansas low still provided the strongest ascending motions due to the strong gradients, but these were dramatically affect by the differential vorticity advection from the divergent wind. The system was nearly vertical with little thermal and vorticity advection from the non-divergent wind around the Kansas low. However, the advection of positive vorticity contributed about 80% of the total omega ahead of the double frontal system.

Second Occlusion Stage - 0000 GMT of 22 February 1976

As expected the fourth map time indicated a general overall decay of total omega values for all three levels (Fig. 23). Again the 900 mb omega pattern becomes elongated in an easterly direction and coincided with a second occlusion as shown in Fig. 10a. Unlike the first occlusion where the omega field regenerated a new omega maximum this pattern showed a weakening low level gradient to the east. Another indication of a decaying system was the nearly vertical alignment of total omega and the zero isopleth for all three levels and a weakening of the omega gradient at the 700 and 500 mb levels.

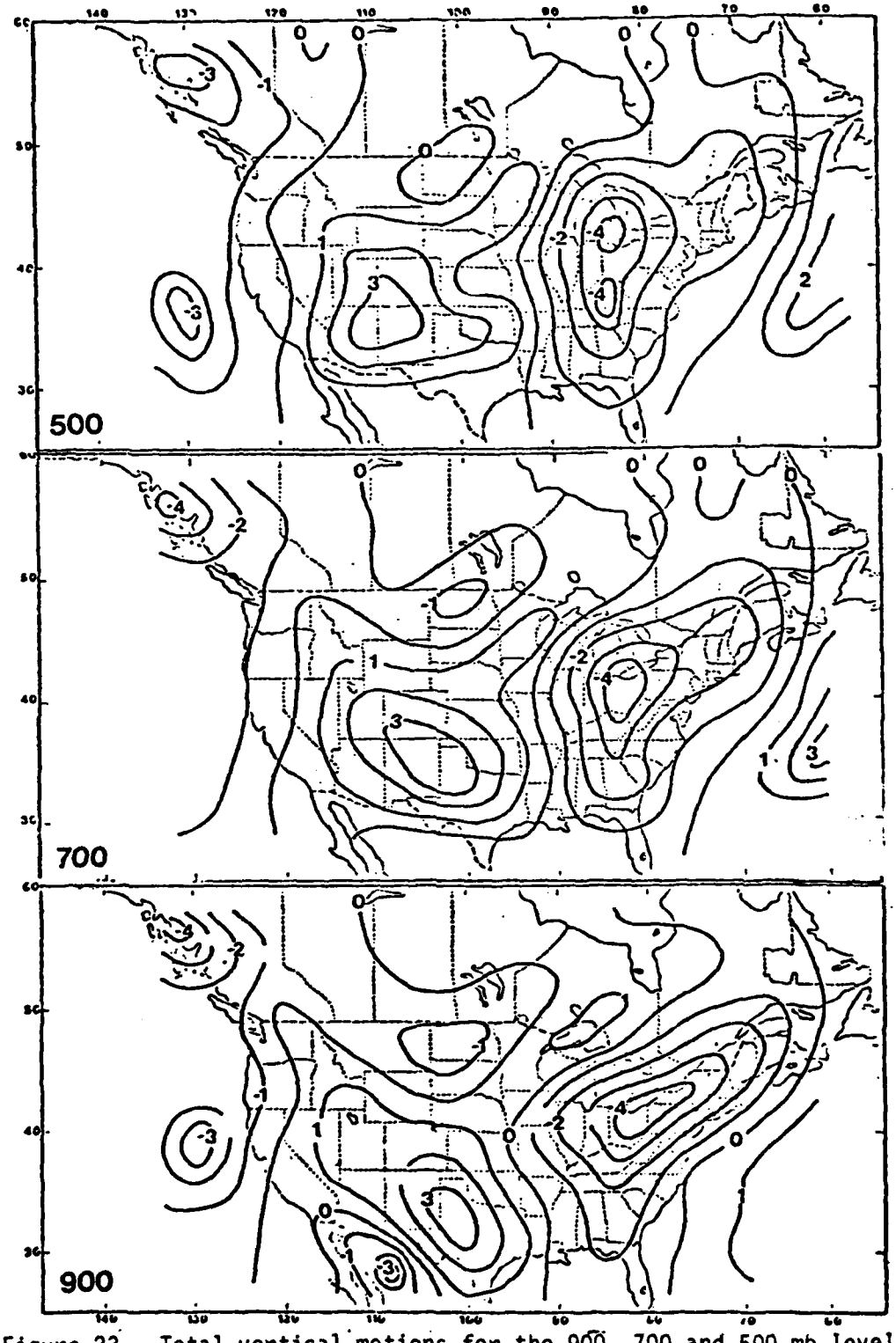

Figure 23. Total vertical motions for the 900, 700 and 500 mb levels at 0000 GMT 22 February 1976. Isopleth interval is 1 $\mu b\ s^{-1}$.

Figure 24 also shows this general weakening of omega gradients at all levels. Upward motions for this system were now lower than in the development stage. The -6 $\mu b\ s^{-1}$ on the west coast was an indication of strong low level westerly flow into the Rockies as another cyclone approached the western United States.

From the 500 mb partitioned omega in Fig. 25, one of the significant features was the warm air advection completely out of phase with the negative vorticity advection at 101°W latitude. This is indicated from the differential vorticity advection and Laplacian of thermal advection, both by the non-divergent part of the wind. The warm air advection behind the upper level trough caused it to tilt in a northeast direction and weaken the entire storm system.

Temperature Fields

The interpolated temperatures received from HIRS radiance measurements correlated, to within a half grid interval, to the synoptic patterns viewed from two geostationary satellite passes. Three orbits of HIRS Nimbus VI data were used in this study as depicted in Fig. 2. To correlate Nimbus VI data with GOES-East visual imagery for 1700 GMT 20 February 1976 (Fig. 27) two successive polar orbital passes were used. The two Nimbus VI orbits were 3397 with a 40°N latitude pass time of 1712 GMT and orbit 3398, which passed 27° west of 3397 with a 40°N latitude pass time of 1859 GMT. This observation time was during the development and intensification stages of the midlatitude cyclone. Path swaths for these two orbits were merged into one map of blackbody radiative temperatures with the objective analysis technique described in Chapter II. These radiation data were obtained from Channel 8 on

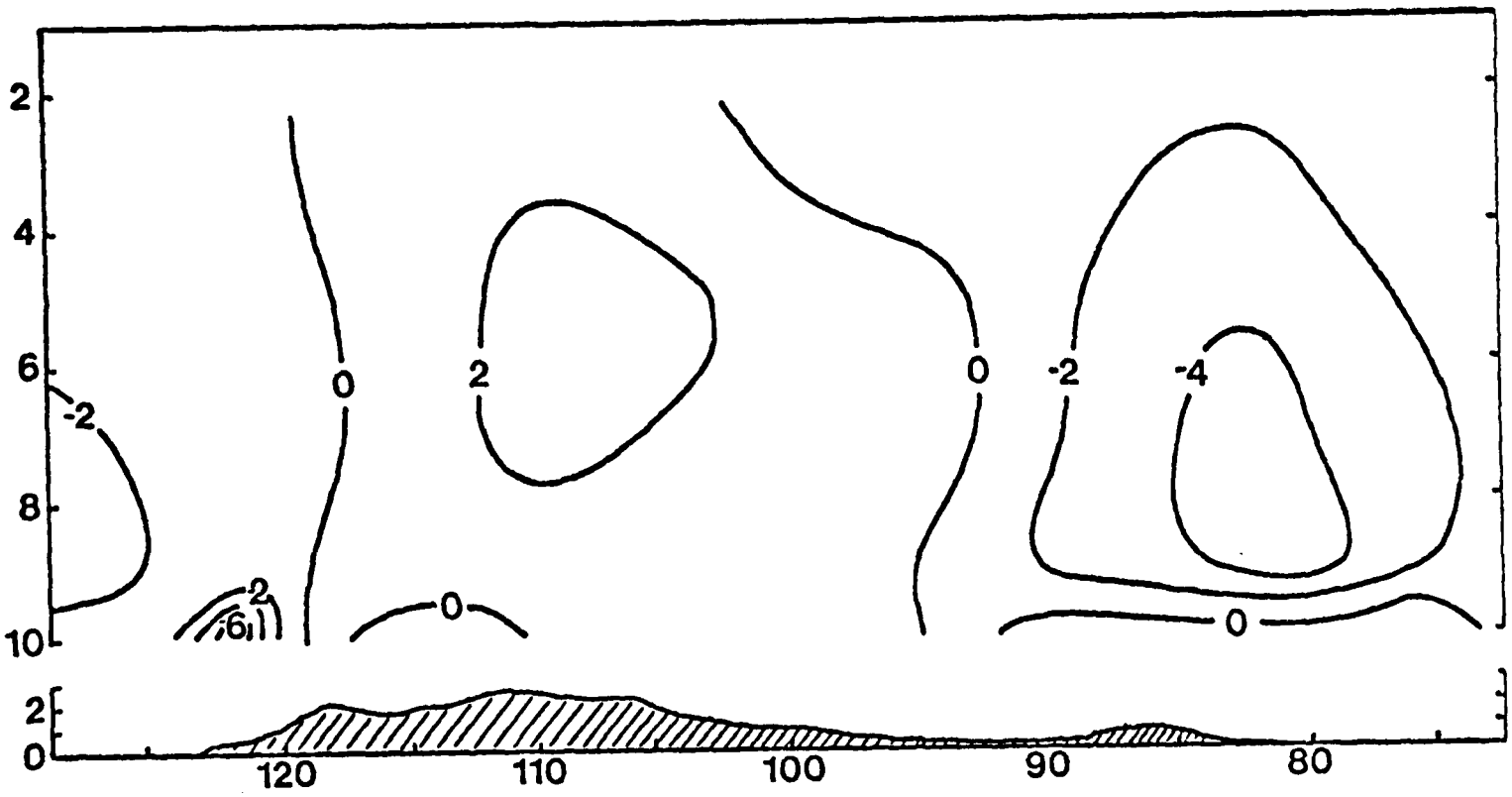

Figure 24. East-West cross-section of total vertical motions along 40°N latitude at 0000 GMT 22 February 1976. Isopleth interval is 2 μb s^{-1}. Ordinate units are 10^2 mb and 10^3 m.

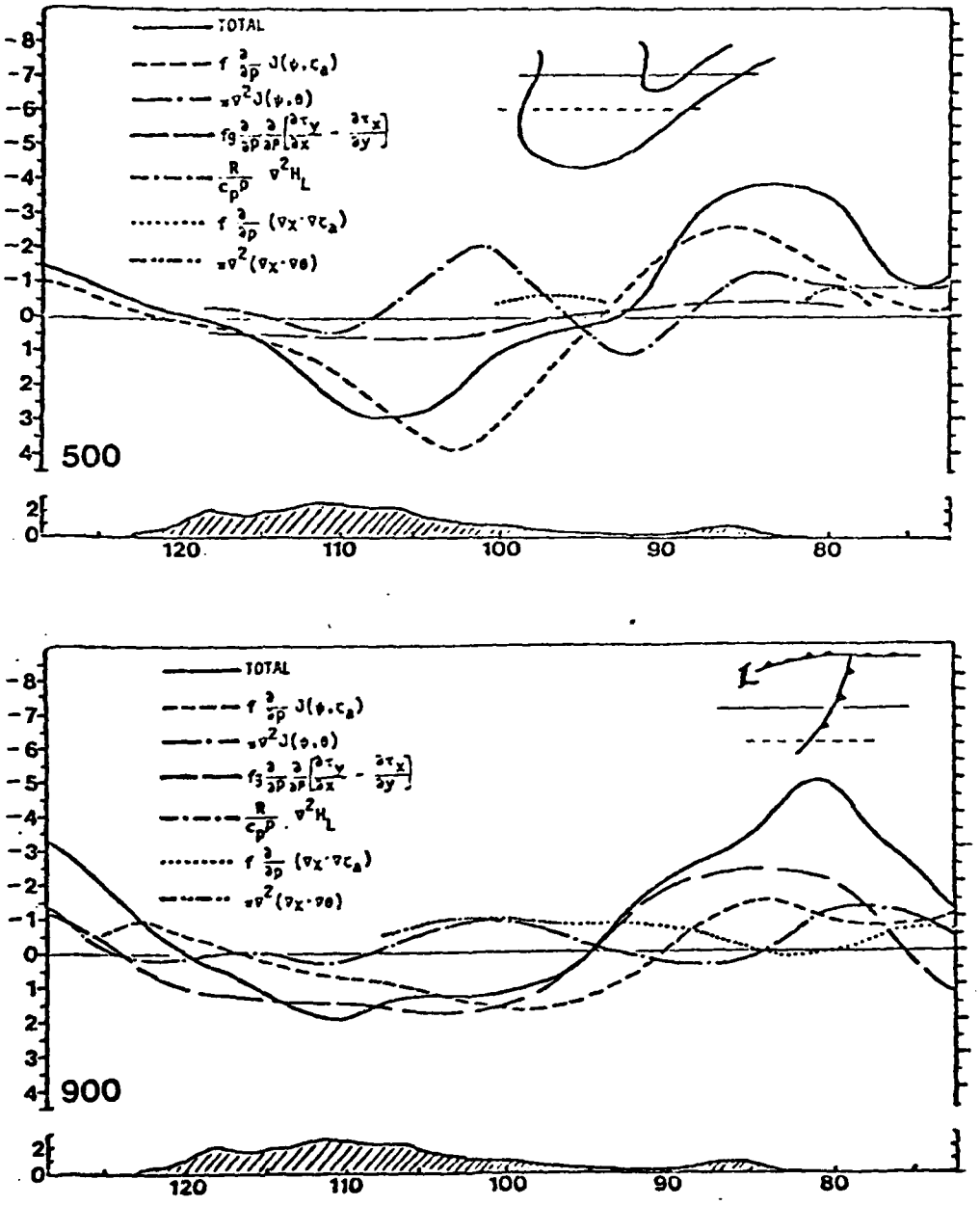

Figure 25. East-West cross-section of 900 and 500 mb partitioned vertical motions along 40°N latitude at 0000 GMT 22 February 1976. Ordinate units are 1 μb and 10^3 m.

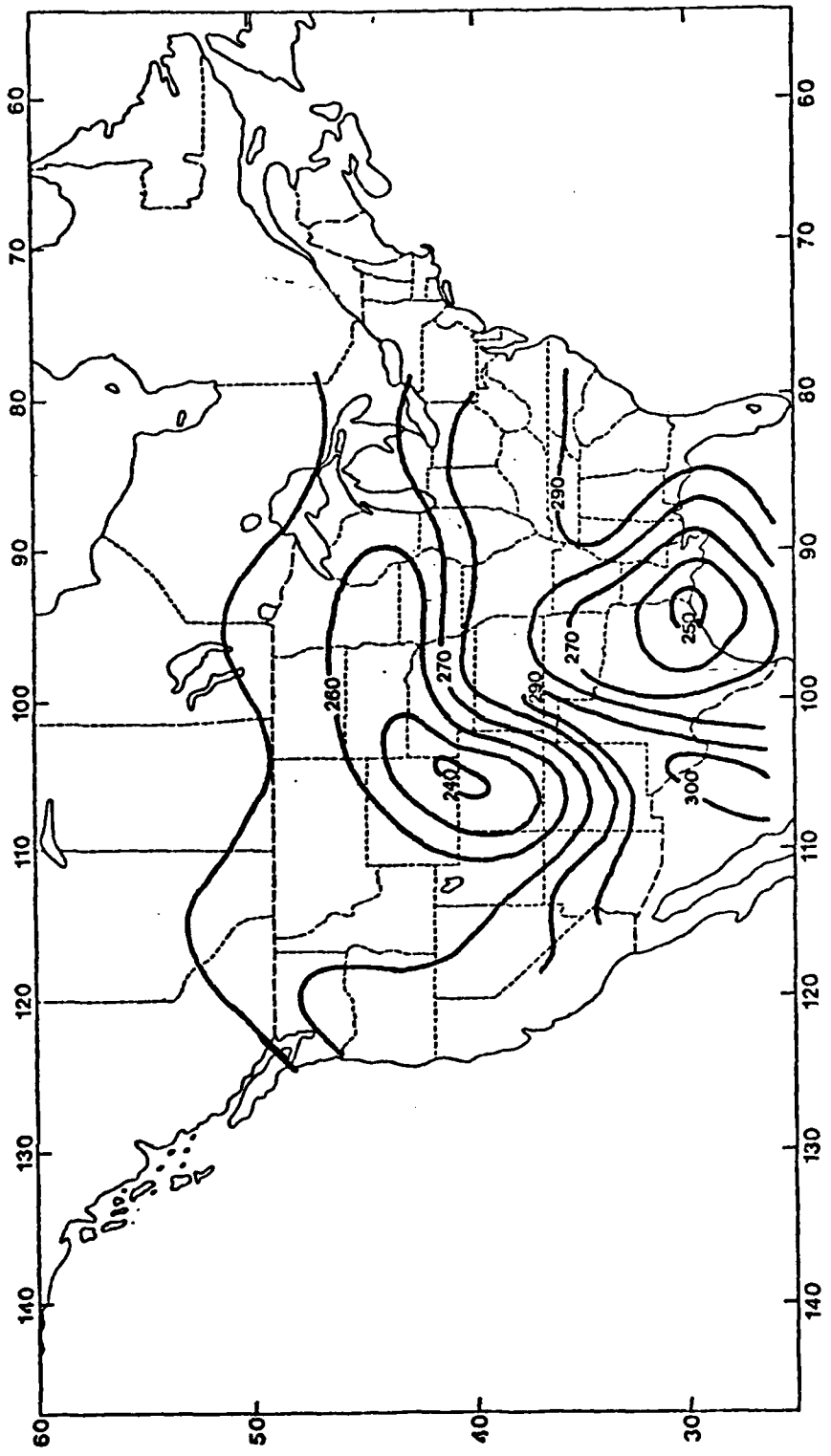

Figure 26. Radiative temperatures from HIRS experiment at 1710 and 1859 GMT 20 February 1976.

Figure 27. GOES-East visual satellite imagery at 1700 GMT 20 February 1976.

the HIRS instrument and represent radiation emitted in the 11.0 μm window region. Therefore, the radiative temperatures approximate surface temperatures in clear areas and cloud top temperatures in overcast areas.

At 1630 GMT on 21 February 1976, orbit 3410 passed through 40°N latitude and coincided with the GOES-East infrared imagery for 1630 GMT (Fig. 29). These data are for the period between the first and second occlusions in the evolution of the cyclone.

Fig. 26 depicts the radiative temperatures in degrees Kelvin from the HIRS data. This pattern conformed very closely to both the cloud and cloudless areas of Fig. 27 in many areas. The wedge of dry air extending from Mexico into Kansas was located over dry land that had very high temperatures. Fig. 26 shows radiative temperatures in excess of 300°K over northern Mexico and as high as 292°K in a narrow band that extended north into Kansas. February 1976 was a record breaking month with temperatures 10 degrees above normal throughout most of the nation and only one intrusion of polar air occurred in the entire month (Weatherwise, 1976).

The area of cold radiative temperatures of less than 240°K or 035°C were located in northern Colorado and southern Wyoming. This area compared favorably with the radar echoes near this map time as depicted in Fig. 3d and was associated with an extensive cloud region northwest of the developing surface cyclone. Comparisons with the 500 mb charts shown in Figs. 3b and 3d indicate the clouds extended above the 500 mb level. The 500 mb temperatures were approximately -30°C in this area.

Fig. 28 shows the infrared temperatures for orbit 3410 when the cyclone was in the occluded stage of development. By this time considerable high clouds had been produced by the convective activity in the warm air secotr, so that much colder temperatures appear in Fig. 28 compared to Fig. 26. Temperatures less than 230°K extended from the Mississippi Valley to Lake Huron and coincided with the band of high clouds shown in Fig. 29 along the cold front.

Adjacent to the frontal cloud band a warm tongue of infrared temperatures extended into northeastern Missouri. This appeared along the western edge of the orbital swath in Fig. 28. The warm tongue was associated with the clear slot behind the cold front and low level cloudiness; however, the ogjectively analyzed temperature field could not resolve this detail.

Further north the cloud band over Iowa and southern Minnesota was associated with the flow north of the 500 mb cyclonic vortex that was located over eastern Kansas on 21 February at 1200 GMT (Fig. 8b). Fig. 28 shows the radiative cloud top temperatures were approximately 245°K. This suggests the presence of high level altostratus or low cirrus clouds in this region and coincides with ascending motion at 500 mb (F9g. 18). Good agreement was also found with the rising motions in Fig. 18 and the infrared temperature over the eastern Great Lakes region. For example, the 240°K isotherm compared favorably with the -1 $\mu b\ s^{-1}$ isopleth of omega.

The warmest temperatures in Fig. 28 were located over the Gulf Stream in the Atlantic Ocean east of the Florida peninsula. Here, temperatures exceeded 290°K. Along the southeastern United States the infrared temperatures in Fig. 28 were warmer than 285°K.

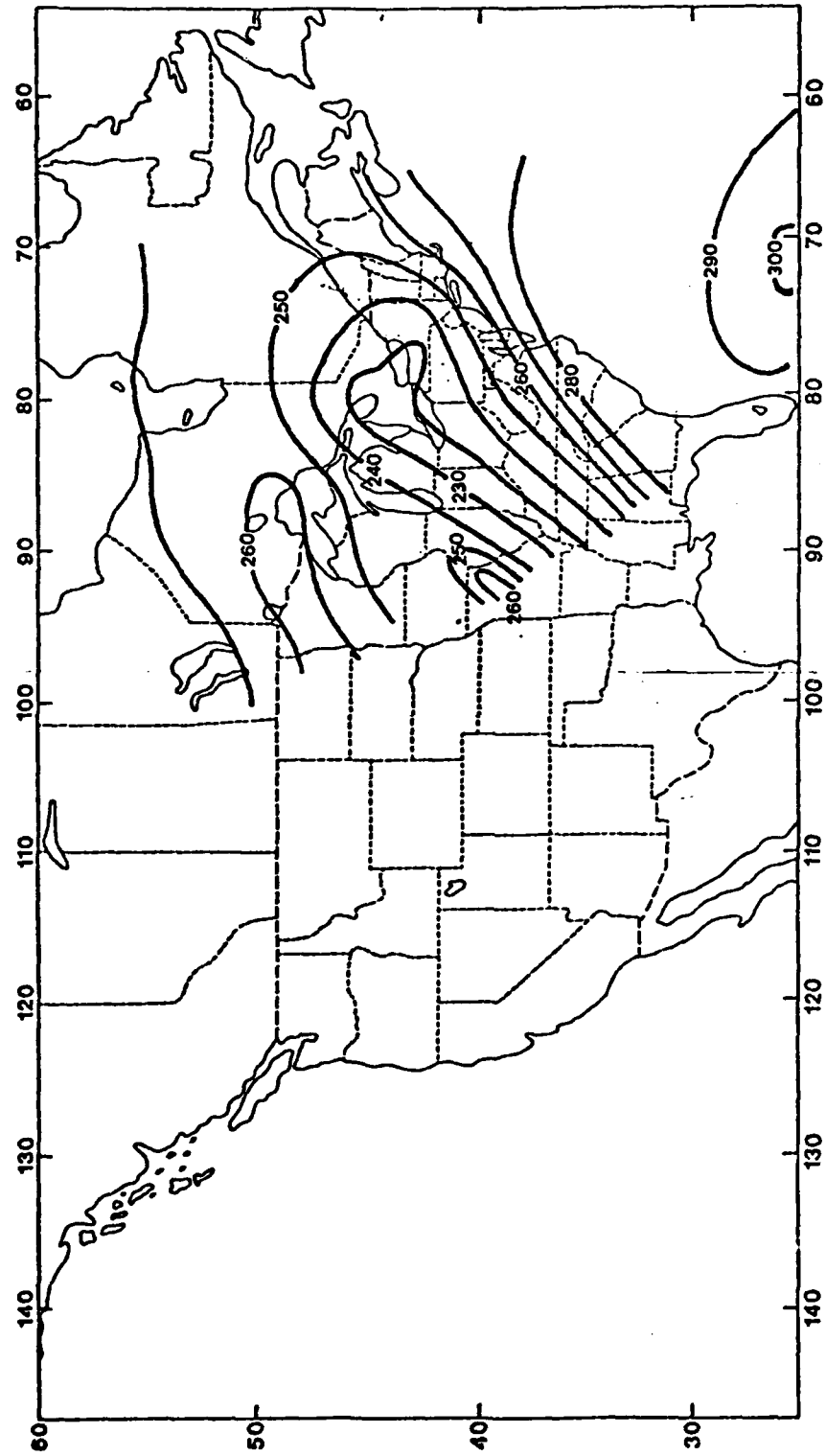

Figure 28. Radiative temperatures from HIRS experiment at 1630 GMT 21 February 1976.

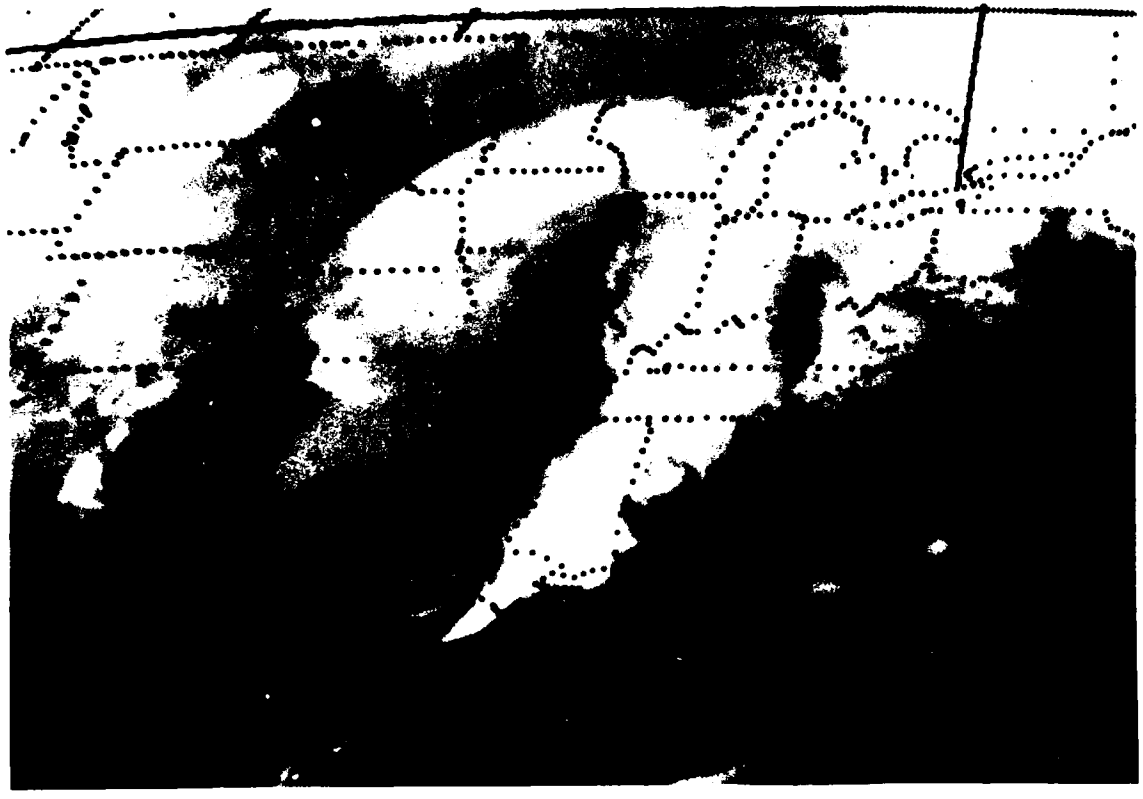

Figure 29. GOES-East infrared satellite imagery at 1630 GMT 21 February 1976.

CHAPTER V

COMPUTATIONAL RESULTS OF THREE DIMENSIONAL TRAJECTORIES

Numerous trajectories were computed for this case study and comparisons were made with satellite data by superimposing trajectories onto GOES satellite picture for various map times during the evolution of the cyclone. This chapter considers moisture flow patterns, areas of wide spread ascending motions of moist air, post frontal subsidence of dry air and vertical wind shears. Except for some subsynoptic cloud patterns many of the satellite cloud images can be explained with the three dimensional trajectories

Computations were made for trajectories starting at the 1000, 900, 800, and 400 mb levels. Various combinations from these levels were applied to the three imagery times -- 0001 GMT, 1200 GMT and 1700 GMT 21 February 1976. The imagery with superimposed trajectories consisted of one visual and two infrared images. One of the infrared pictures was enhanced in order to distinguish variations in the cloud top temperature of a cirrus shield.

GOES-East Enhanced Imagery at 0000 GMT 21 February 1976

The most dramatic aspect of this image (Fig. 30) was the organized prefrontal line of severe weather which occurred on the western edge of low level moisture influx that was previously discussed and shown in Figs. 7a and 7b. This convective activity was well defined in the enhanced infrared image. Cloud top temperatures of the convective anvil

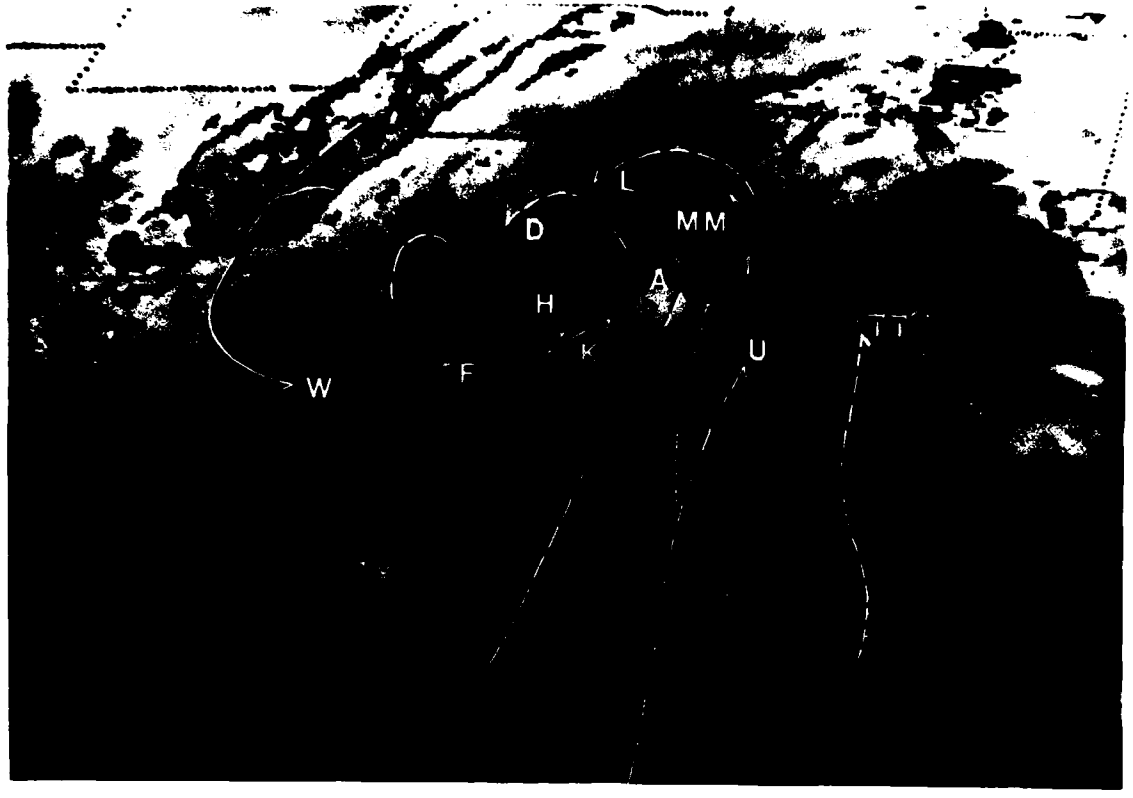

Figure 30. GOES-East enhanced satellite imagery at 0001 GMT 21 February 1976 with 12 hour superimposed trajectories for (a) 1000 mb level.

cirrus were colder than -59°C for the black contoured region shown in Fig. 30a (area 2). Much colder cloud top temperatures (<-65°C) were imbedded within this convective cloud line and were indicated by the white contoured area shown in Fig. 30a (area 1).

This section will examine some specific trajectories that appeared to contribute to the development of the convective cloud line and the surrounding areas for the 1000, 800, and 400 mb levels. Although the contoured area was an integral part of the synoptic situation, it was considered here as a mesoscale system partly due to the rapid formation and subsequent dissipation. Also, the width of the entire convective cloud area was less than the east-west grid size and, as a result, this mesoscale feature may not have been completely resolved by the grid network used in this study.

Table 1 summarized some of the 12 hour trajectories that ended at 0000 GMT 21 February 1976. This table gives the pressure height of 25 different trajectories at 4 hour time increments. The horizontal position of these trajectories were superimposed on the GOES infrared pictures for 0001 GMT 21 February 1976 and are identified in Fig. 30 by alpha numeric symbols used in Table I.

It can be seen that some trajectories start at the same grid point but at different pressure levels. For example, 2 trajectories began at the 1000 and 800 mb levels at 27.5°N latitude and 97.5°W longitude (which is designated by point A) in Figs. 30a and 30b. For the point at the 1000 mb level the flow was southwesterly and was converging with southeasterly flow to the east in the prefrontal cloud region. Table 1 shows point A experienced a 74 mb ascent during this 12 hour period. However, at higher levels the flow is more westerly.

Table 1. Pressure levels for twelve hour trajectories ending at 0000 GMT 21 February 1976. Horizontal positions are superimposed on GOES satellite imagery in Fig. 30, the +12 hour time step corresponds to the satellite picture time in Fig. 30. Asterisks denote air parcels that originated outside the picture area.

Point	Int. Press	+4 Hour	+8 Hour	+12 Hour	Map
A	1000	981	949	926	30a
D	"	917	848	793	"
F	"	941	897	871	"
H	"	961	927	900	"
K	"	968	940	925	"
L	"	954	877	771	"
U	"	998	992	973	"
W	"	965	966	974	"
X	"	983	968	940	"
MM	"	979	948	897	"
TT	"	998	995	982	"
A	800	783	758	727	30b
E	"	743	708	688	"
F	"	744	691	640	"
H	"	759	715	658	"
M	"	767	732	683	"
O	"	799	802	802	"
P	"	781	760	740	"
W	"	764	757	784	"
G	400	387	380	380	30c
R *	"	419	430	436	"
S *	"	412	417	410	"
T *	"	440	459	479	"
Q *	"	398	387	352	"
X	"	366	345	332	"
XX	"	397	386	374	"
YY	"	389	387	394	"

When point A was started at the 800 mb level, it crossed over the lower level flow and ascended by 73 mb. Point A in Figure 30a also shows the inflow of warm moist air from the Gulf of Mexico, to the thunderstorm area of maximum intensity in northeastern Oklahoma. Points U and TT located to the east of Point A moved northward, and did not spiral into the low pressure circulation. Table 1 indicates U and TT experienced small ascending motions of only 18 and 27 mb, respectively. These two parcels eventually provided moisture influx to the area of precipitation which occurred around the occluded system after the severe weather dissipated.

Another interesting trajectory in Fig. 30a and Table 1 was point L which spiraled around the surface low vortex in central Kansas and ascended from 1000 to 771 mb in 12 hours. Points L and D were located in the low level easterly flow north of the cyclone center and compared favorly with the low level cloud field that "wrapped around" the surface low on its poleward side.

Inflow of dryer air from the southwest was evident from points F, H, K and BB in Fig. 30a. Point K experienced the smallest ascent (75 mb) in the southerly flow ahead of the cold front shown in Fig. 6a. The displacement of parcels F, H, D and W was representative of the low level trough in the eastern Oklahoma panhandle (Fig. 6a) which provided some impetus for the rapid development of the severe weather system. A weak area of postfrontal subsidence is seen at point W in Fig. 30a. The rising motion in the first four hour time step for the W trajectory was primarily upslope induced due to the low center circulation in Kansas.

For the trajectories that started at 800 mb (Fig. 30b), the low

Figure 30. (b) 800 mb and

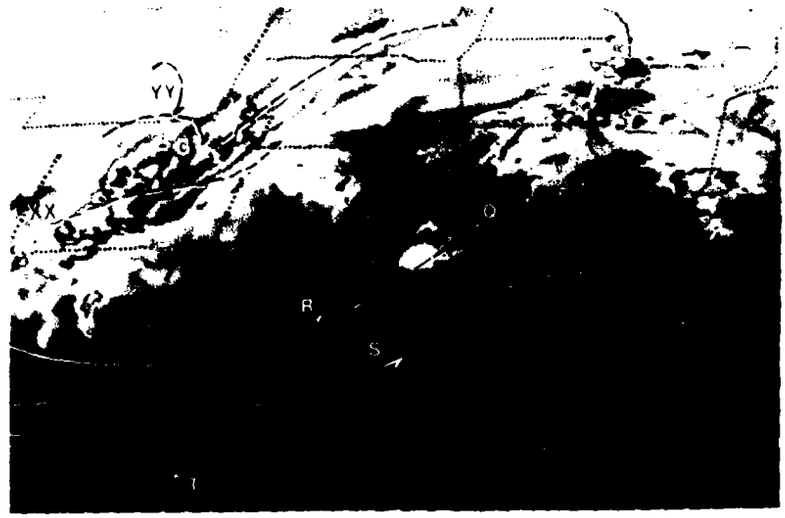

Figure 30. (c) 400 mb levels.

Figure 30. (b) 800 mb and

Figure 30. (c) 400 mb levels.

level trough is readily identified from points F, E and W. Of these three, F showed the strongest rising motion with 160 mb ahead of the trough while E was displaced upward by 112 mb. Point W experienced ascent for the first 8 hours and coincided with the initial 4 hour trajectory path at 1000 mb. Both of these trajectories were parallel to the northeast-southwest cloud band extending over Nebraska and Colorado. Fig. 30b shows cloud top temperatures decreased along the rising portion of the trajectory path of point W and increased along the sinking portion.

The 800 mb flow in the vicinity of the severe thunderstorm cells in Fig. 30b was primarily a westerly component with southwesterly flow in the prefrontal area over the lower Mississippi River Valley region. The rapidly rising air at point H ascended from 800 to 658 mb in 12 hours into the large storm vortex (Table 1). The rising air extended all along the prefrontal cloud band with a 60 mb ascending motion at point P until the first area of subsidence was found at the southern extent of clouds at point O.

In Fig. 30c westerly parcel motion at the 400 mb level was also evident through the severe thunderstorm line. The subsidence area extended behind the prefrontal cloud band and was supported by trajectories R, T and S. Sinking motion for S ended four hours before the imagery time and prior to the rapid development (Table 1) and then was followed by rising motion. The greatest ascent by these trajectories was represented by parcel Q. Its path went through the intense cell in southern Oklahoma. This trajectory ascended by only 13 mb before it reached the convective cloud band and then was displaced upward by more than 35 mb in a four hour time interval within the cloud region.

The contoured cloud map extending from Colorado into South Dakota was located in the downwind flow of the upper level trough. The trough axis can be positioned with the rising motions at point XX and the sinking motion of points G and YY (Table 1). This cloud pattern was the cirrus blow off from the Colorado buildups induced from the low level easterly flow of points E and W in Figs. 30a and 30b.

GOES-East Infrared Imagery at 1200 GMT 21 February 1976

Twelve hours later an occluded low level system and a dry tonque extended through Missouri. Trajectories associated with these two features are depicted in Fig. 31 and Table 2. Comparing the low level parcel paths of points AA and Y from 1000 and 900 mb (Figs. 31a and 31b) it is apparent that the dry tongue subsidence extending all the way to the occluded front in Missouri was from parcels that originated below 900 mb. These parcels on Fig. 31a experienced rising motions into the severe weather system until the storm quickly decayed by 0400 GMT and then they provided the subsident motion into the dry tongue behind the cold front.

In Fig. 31b, the 900 mb subsiding air at Y, Z, AA and BB was positioned very near to the western extent of the cold front (Fig. 8a) which was underlying the cirrus shield over the Mississippi Valley. Even the next four hour period indicated a sinking motion behind the front as it moved eastward (Table 2 and 4). The parcel at H underwent rising motion throughout its entire history and eventually moved into the upper level trough.

The low level subsidence behind the rapidly moving cold front was evident even at 800 mb from points CC, DD and Y (Fig. 31c). Those

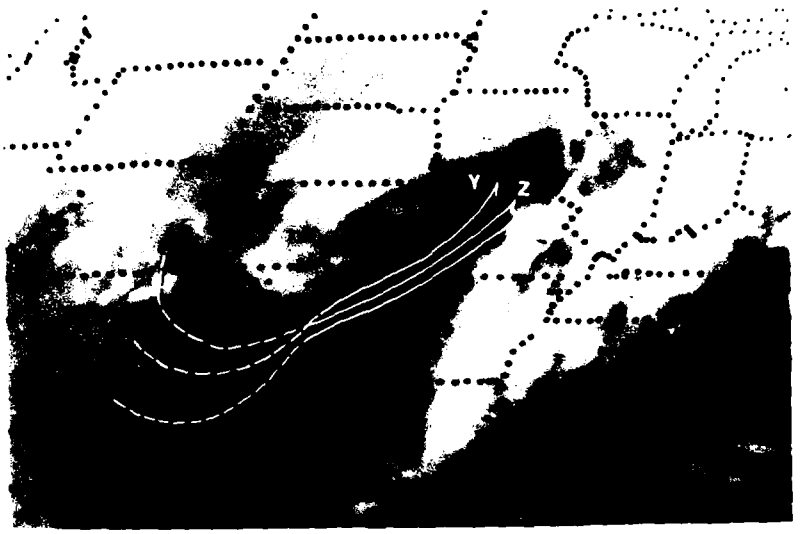

Figure 31. GOES-East infrared satellite imagery at 1200 GMT 21 February 1976 with 24 hour superimposed trajectories for (a) 1000

(b) 900 mb levels

Table 2. Pressure levels for twenty-four hour trajectories ending at 1200 GMT 21 February 1976. Horizontal positions are superimposed on Fig. 31. The +24 Hour time step corresponds to the satellite picture time in Fig. 31. Asterisks denote air parcels that originated outside the picture area.

Point	Int. Press	+4 Hour	+8 Hour	+12 Hour	+16 Hour	+20 Hour	+24 Hour	Map
Y	1000	997	991	985	973	991	996	31a
Z	"	982	977	978	969	993	1000+	"
AA	"	990	980	969	954	978	1000+	"
H	900	861	823	785	734	697	674	31b
Y	"	897	889	883	867	887	951	"
Z	"	882	874	878	876	895	961	"
AA	"	890	879	862	837	853	903	"
BB	"	883	868	834	801	802	826	"
Y	800	796	787	782	762	769	801	31c
CC	"	787	770	757	727	719	722	"
DD	"	784	765	756	735	734	755	"
EE	"	781	760	750	740	749	790	"
FF	"	777	753	727	682	647	614	"
GG	"	774	744	717	673	642	626	"
HH *	400	427	461	504	529	541	554	31d
JJ *	"	418	436	460	468	468	470	"
KK	"	415	434	461	484	500	533	"
LL	"	408	412	417	413	406	404	"
WW *	"	428	456	487	498	496	496	"

Figure 31. (c) 800 mb and

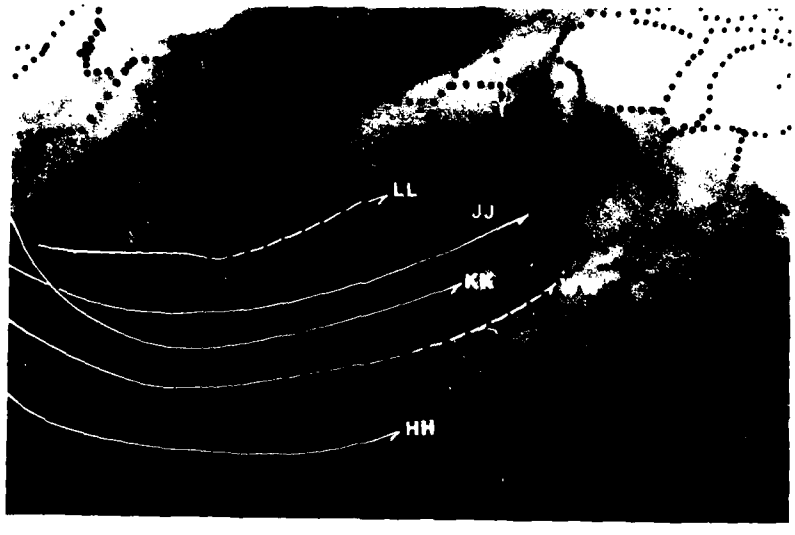

Figure 31. (d) 400 mb levels.

three parcels all underwent lifting of 38 to 81 mb (Table 2) during the severe weather at 0000 GMT; however, in the last four to eight hours the cold front moved from Oklahoma and Kansas to the Mississippi River Valley. The parcels at FF and GG are caught in the cyclonic circulation of the nearly vertical system and move northeastward with good ascending motions of 186 and 174 mbs, respectively (Table 2).

The 400 mb trajectories (Fig. 31d) coincided very well with the cirrus patterns around the Kansas occluded system and the rapidly moving cold front. The cloud band that extended from northern Oklahoma to Iowa consisted mainly of low level clouds wrapping around the vertical circulation center in eastern Kansas. The southern extent of the cirrus overlying the low level moisture band was well defined by point LL, while the eastern edge of the dry tongue was positioned at the subsiding points JJ, KK and HH. During the next four hour period all of these parcels underwent ascending motion (Table 4). Rising motions above the cold frontal system were evident from point WW (in Fig. 31d) which exhibited practically no vertical displacement in the preceding eight hours (Table 2).

GOES-East Visual Imagery at 1700 GMT 21 February 1976

The last of the trajectory sequences depicts the fully developed occlusion, dry tongue and cold frontal cloud band. Comparison of the 1630 GMT infrared and 1700 GMT visual imagery (Figs. 29 and 32) clearly illustrate the two distinct cloud layers over the Oklahoma - Kansas - Missouri borders. The surface low present in this area at 1200 GMT decayed and was filling. From the two sets of trajectories in Fig. 32 it is possible to see the vertical wind shear from 1000 to 900 mb. Six

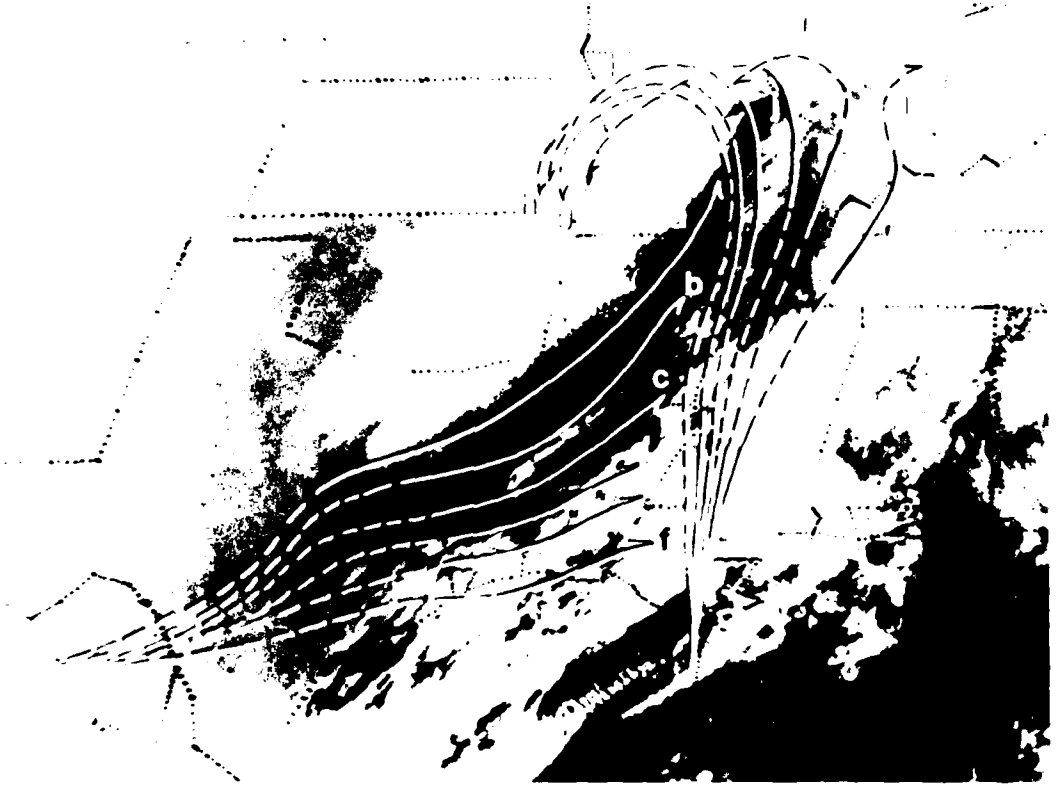

Figure 32. GOES-East visual satellite imagery at 1700 GMT 21 February 1976 with 29 hour superimposed trajectories for 1000, 980, 940, 920 and 900 mb levels.

trajectories were computed at two grid points.

The trajectories originated between 1000 and 900 mb and were separated by 20 mb pressure increments (Table 3). The 900 mb omegas were used for each trajectory computation, and only the horizontal wind component varied according to the interpolation scheme discribed in Chapter II. Inflow to the Kansas low was provided by parcels from 1000 to 920 mb while the 900 mb trajectory followed a path into the Illinois and Indiana low. The dry tongue low-level subsidence was well defined at points a-d from 1000 to 900 mb. These trajectories show the significance of low level flow especially within 50 mb of the underlying surface in determining the low level cloud configurations. At somewhat higher levels there was considerably less agreement with the atmospheric motions and the cloud distribution.

Figures 33a-d and Table 4 illustrate the trajectories from the individual layers. The low level vortex was easily identifiable on Fig. 33a from points BB, NN and PP and was so shallow in vertical extent that the 900 mb (Fig. 33b) shows cyclonic circulation only at point Y. The 1000 mb circulation was intense enough to advect air from Kentucky westward to the Nebraska- Iowa - Missouri border (Fig. 33a, point OO). This parcel ascended 250 mb in the past 24 hour period.

The dry tongue at 900 mb (Fig. 33b) is well identified by the descending motion of point Y and MM. It is interesting to examine the vertical motion associated with points NN and U (Table 4). Although both parcels show rising motion into the cyclones center in Indiana, five hours earlier when the parcels were at 1200 GMT their sinking motion precisely positioned the placement of the eastward moving cold front on the Illinois - Indiana - Kentucky border extending southward

Table 3. Pressure levels for thirty-two hour trajectories ending at 2000 GMT 21 February 1976. Horizontal positions of interpolated twenty-nine hour trajectories are superimposed on GOES satellite imagery in Fig. 32. The +28 hour and +32 hour time steps are used to interpolate the +29 hour picture time of 1700 GMT 21 February 1976 in Fig. 32.

Point	Int. Press	+4 Hour	+8 Hour	+12 Hour	+16 Hour	+20 Hour	+24 Hour	+28 Hour	+32 Hour	Map
a	1000	986	971	942	902	910	981	1000+	1000+	32
b	980	966	952	922	883	885	941	996	1000+	"
c	960	946	931	901	864	861	902	943	962	"
d	940	926	911	880	847	843	873	900	915	"
e	920	907	891	861	832	830	851	868	879	"
f	900	886	872	844	819	818	834	845	853	"
g	1000	1000+	1000+	1000+	987	986	951	920	918	32
h	980	983	987	990	980	981	960	910	906	"
i	960	963	967	972	965	965	967	907	900	"
j	940	943	947	953	949	947	962	907	886	"
k	920	923	928	933	932	928	939	902	866	"
l	900	903	908	914	914	910	915	887	842	"

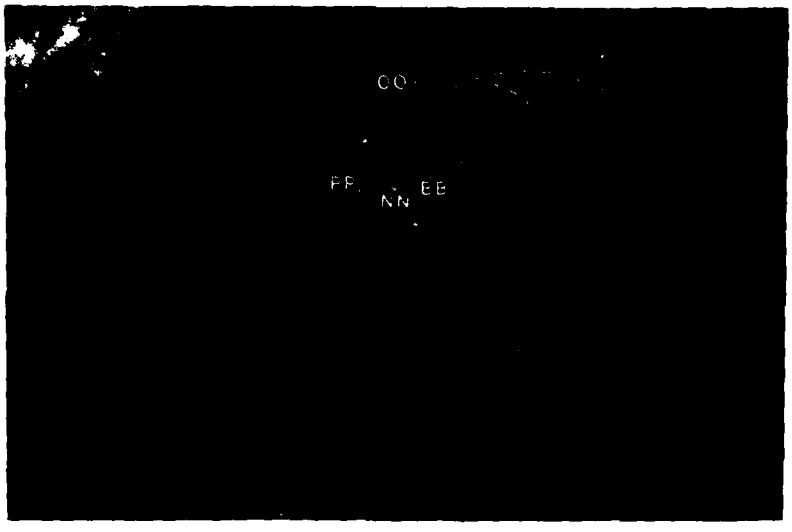

Figure 33. GOES-East visual satellite imagery at 1700 GMT 21 February 1976 with 20 hour superimposed trajectories for (a) 1000 and

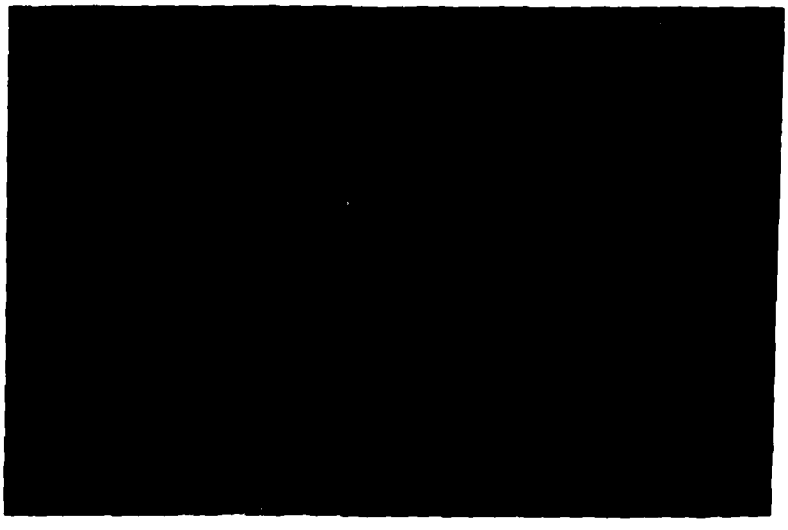

(b) 900 mb levels

Table 4. Same as Table 3 except the table refers to Fig. 33a-33d.

Ident.	Int. Press	+4	+8	+12	+16	+20	+24	+28	+32	Fig.
BB	1000	983	968	940	912	935	1000	1000+	968	33a
NN	1000	1000+	1000+	1000+	987	986	951	920	918	"
OO	1000	1000+	991	930	857	803	773	750	749	"
PP	1000	1000+	989	949	906	868	823	808	809	"
Y	900	897	889	883	867	887	951	1000	981	33b
D	900	817	740	671	625	600	585	567	571	"
MM	900	890	879	862	837	853	903	937	939	"
NN	900	903	908	914	913	910	915	887	842	"
U	900	898	894	887	869	866	869	824	769	"
DD	800	784	765	756	735	734	756	757	738	33c
QQ	800	784	764	752	722	712	713	687	643	"
Y	800	796	787	782	762	769	801	809	795	"
AA	800	787	775	757	725	719	721	698	662	"
BB	800	784	773	751	726	720	724	713	693	"
WW	400	428	456	487	498	496	495	453	402	33d
JJ	400	418	436	460	468	469	470	431	394	"
KK	400	415	434	461	484	499	533	522	485	"
RR	400	400	403	417	434	455	485	516	536	"
SS	400	400	404	417	439	468	496	523	549	"

along the Mississippi River.

The 800 mb trajectories on Fig. 33c show an approximate position of the surface front when the subsidence of parcels DD, AA, Y and BB change to ascending motions by comparing Fig. 8a and 10a.

The five points at the 400 mb level accurately depict the cloud formation over the central United States (Fig. 33d). The southern edge of the cirrus streak through northern Missouri and Iowa is traced with parcel JJ (Fig. 29). Points KK and SS outline the western edge of the cold front cirrus blow off pattern while points RR and SS mark the extent of the subsidence in the dry tongue.

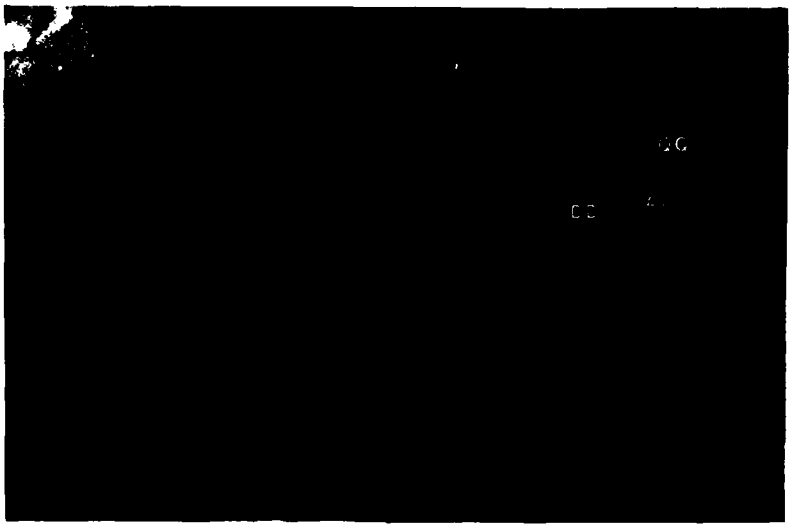

Figure 33. (c) 800 mb and

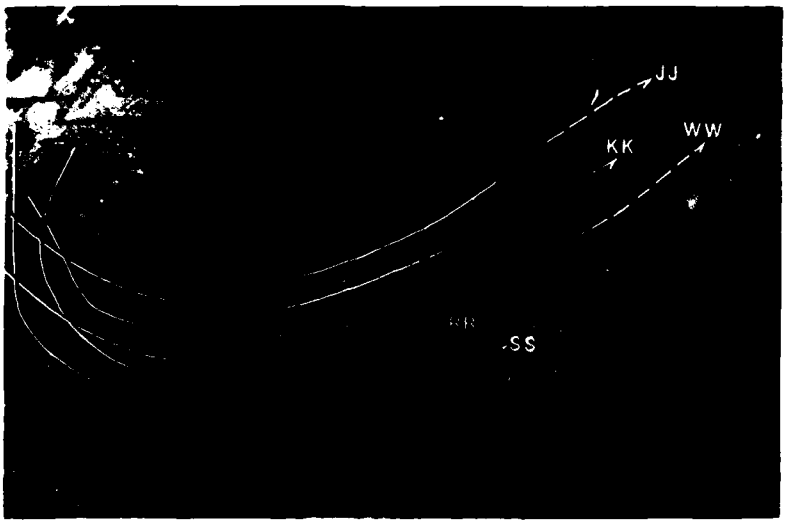

Figure 33. (c) 400 mb levels.

CHAPTER VI

CONCLUSION

In this study a detailed dynamic and synoptic investigation was carried out for a mid-latitude cyclone. A time sequence of analyzed synoptic charts and numerical computations were combined with polar orbiting and geostationary satellite data in order to consider various physical and dynamical mechanisms that were associated with the evolution of the storm.

Results of this study indicated that the Laplacian of thickness advection and differential vorticity advection by the nondivergent part of the flow, together with surface fractional effects, were the dominate mechanisms throughout the life history of the cyclone. The storm underwent rapid development when the ascending motions, produced by these forcing functions, were nearly coincident and exhibited no vertical tilt in the lee of the Rocky Mountains. When the cyclone reached maturity, the strongest thermal and vorticity effects at mid-tropospheric levels advanced eastward ahead of the most intense frictional components at low levels. When the cyclone began to occlude, sinking motion was contributed by differential vorticity advection by the divergent part of the flow at low levels. This effect decreased the strong rising motion due to friction and eventually produced a shallow layer of subsidence that extended into the occluded system.

Numerical computations of three dimensional trajectories

illustrated the importance of low level moisture flow and the development of intense convective activity within the warm air sector of the cyclone. Comparisons of atmospheric trajectories with visible and infrared imagery from satellites showed good agreement with cloud fields and vertical motions. Also, the numerical computations showed the importance of low level flow in determining the configuration of cloud fields on a synoptic scale.

APPENDIX

LIST OF SYMBOLS

Symbol	Description of Symbol
σ	Dry static stability
ω	Vertical velocity
f	Coriolis parameter
p	Pressure, vertical direction
T	Air temperature
J	Jacobian operator
ζ_a	Absolute vorticity
π	Symbol of $RT/p\theta$
∇^2	Laplacian operator
ψ	Non-divergent part of the wind
θ	Potential temperature
τ_x, τ_y	Frictional stresses
c_p	Specific heat of air at constant pressure
R	Gas constant
H_L	Latent heat release due to stable and convection mechanisms
χ	Divergent part of the wind
x	East-west direction
y	North-south direction

REFERENCES

Astling, E. G., 1976: Some Aspects of Cloud and Precipitation Features Associated with a Midlatitude Cyclone. Monthly Weather Review, 104, 1466-1473.

Berkofsky, L., and E. A. Bertoni, 1960: Topographical Charts at One Degree Intersections for the Entire Earth. Rep. No. 42, Geophysical Research Directorate, AFCRL, Bedford, Mass., 28 pp.

Cressman, G. P., 1959: An Operational Objective Analysis System. Monthly Weather Review, 87, 367-374.

Danielsen, E. F., 1973: Review of Trajectory Methods. Advance in Geophysics, 18, 73-94.

Jenne, R. L., 1970: The NMC Octagonal Grid. Report by National Center of Atmospheric Research, Boulder, Colorado, 14 pp.

Krishnamurti, T. N., 1968a: A Diagnostic Balance Model for Studies of Weather System of Low and High Latitudes, Rossby Number less than 1. Monthly Weather Review, 96, 197-207.

_____, 1968b: A Study of a Developing Wave Cyclone. Journal Applied Meteorology, 9, 942-946.

Palmén, E, and C. W. Newton, 1969: Atmospheric Circulation Systems, Academic Press, New York, 344-350.

Reap, R. M., 1972: An Operational Three-Dimensional Trajectory Method. Journal Applied Meteorology, 11, 1193-1202.

Staff Members, 1975: Nimbus VI User's Guide, Goddard Space Flight Center, NASA, Greenbelt, Md., 227 pp.

Staff Members, 1976: Weatherwatch, Weatherwise, 29, 94-111.

AD-A107 986 AIR FORCE INST OF TECH WRIGHT-PATTERSON AFB OH F/G 4/2
A DYNAMIC AND SYNOPTIC STUDY OF A WINTERTIME CYCLONE USING GEOS--ETC(U)
JUN 79 J A HALL
UNCLASSIFIED AFIT-CI-79-281T-S NL

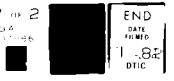

Name

Birthplace

Birthdate

High School

Universitie
1961-1

1968-1

1970-1

1972-1

1977-1

Degrees
1974

Honorary Sc

Professiona

VITA

John Andrew Hall

Wadena, Minnesota

June 4, 1943

Wadena High School
Wadena, Minnesota

University of Minnesota
Minneapolis, Minnesota

University of Arizona
Tucson, Arizona

Parkland College
Champaign, Illinois

St. Louis University
St. Louis, Missouri

University of Utah
Salt Lake City, Utah

B.S., St. Louis University

Chi Epsilon Phi

Weather Officer
United States Air Force

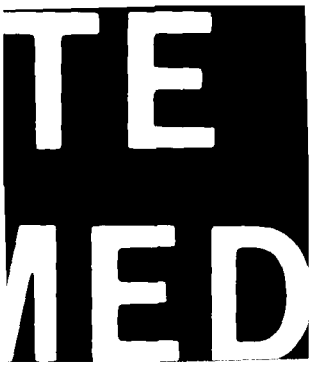
TE
ED